AD_____

Award Number: DAMD17-01-1-0090

TITLE: Targeted Delivery of Therapeutic Oligonucleotides for the Treatment of Prostate Cancer

PRINCIPAL INVESTIGATOR: Song Li, M.D., Ph.D.

CONTRACTING ORGANIZATION: University of Pittsburgh
Pittsburgh, Pennsylvania 15260

REPORT DATE: May 2004

TYPE OF REPORT: Final

PREPARED FOR: U.S. Army Medical Research and Materiel Command
Fort Detrick, Maryland 21702-5012

Table of Contents

INTRODUCTION:

Androgen independence and chemoresistance are the major obstacles in the treatment of patients with advanced prostate cancer (Denis & Murphy, 1993; Oh & Kantoff, 1998). Recent studies have suggested that overexpression of a proto-oncorprotein, Bcl-2, plays an important role in the development of androgen independence and chemoresistance in prostate cancer (McDonnell et al., 1992; Colombel et al., 1993; Berchem et al., 1995; Raffo et al., 1995; Bauer et al., 1996, McConkey et al., 1996). We propose in this application to develop a tumor-specific vehicle to selectively deliver to the tumor an antisense oligodeoxynucleotides (ODN) that is targeted to Bcl-2. Down-regulation of Bcl-2 in prostate cancer could render it more susceptible to the standard chemotherapy. Sigma receptor will be chosen as the target as they are overexpressed in a number of tumors including prostate cancer (Vilner et al., 1995; John et al., 1993; John et al., 1995a; John et al., 1995b; John et al., 1996; John et al., 1999a; John et al., 1999b).

BODY:

Two specific aims were originally proposed in our application and a three-year support was requested. A two-year support was later approved to request us to focus on the first aim: ***to develop novel delivery systems for targeted delivery of ODN to prostate cancer.*** Two issues are critical for achieving this goal: 1) to identify a targeting ligand that is highly specific for prostate cancer; and 2) to develop a lipid vector that is highly efficient in encapsulating ODN and in mediating selective delivery of ODN to target cells. Accordingly, we have developed two different types of tumor-specific ligands, i.e., anisamide derivative and D-βE peptide that are targeted to sigma receptor and prostate specific membrane antigen (PSMA), respectively. Both ligands are efficient in mediating liposomal targeting to prostate cancer cells. In addition, we have developed a new method that is highly efficient in encapsulating ODN inside lipidic vector and in mediating intracellular delivery of ODN in cell-type-specific manner. Three papers have been published as a result of the above studies. The following highlights the major findings from these studies.

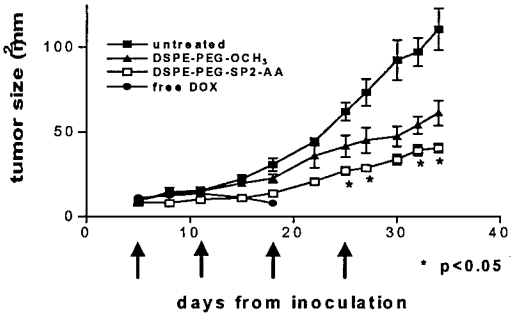

Fig. 1. Inhibitory effect of anisamide-targeted liposomal DOX on the growth of DU-145 tumor. Groups of five mice were inoculated with DU-145 cells. Five days later mice received the following treatments at a DOX dose of 7.5 mg/kg: A) DOX-liposome containing DSPE-PEG(2000)-OCH_3 (black triangle); B) free DOX (black circle); and C) DOX-liposome containing DSPE-PEG-SP2-AA (white square). Control mice received HBS. Tumor sizes in each group were measured twice a week and compared. *P<0.05 (vs DOX-liposome containing DSPE-PEG(2000)-OCH_3). Free DOX treatment was terminated at day 22 because all mice died of toxicity.

1. Targeted delivery of liposomal drugs to prostate cancer cells: In collaboration with Dr. Leaf Huang, we

have recently shown that anisamide-derivatized ligand efficiently mediates delivery of liposomal doxorubicin (DOX) to DU-145 prostate cancer cells that overexpress sigma receptor in vitro and in vivo (Banerjee, R., Tyagi, P., *Li, S., & *Huang, L., *International Journal of Cancer, in press*). Targeted DOX delivery not only improved the antitumor activity but also decreased the DOX-related toxicity (Fig. 1). More recently we have shown that a small molecule glutamate carboxypeptidase inhibitor (DβE) also efficiently mediates liposomal targeting to LNCaP cells that overexpress PSMA. Figure 2 shows the uptake of the rhodamine (Rho)-labeled liposomes 1 h following incubation with LNCaP cells at 37°C. DβE-conjugated liposomes were more efficiently taken up by LNCaP cells than the control non-targeted liposomes. Liposomal targeting appears to be specifically mediated by PSMA because there is only a background level of liposomal uptake in DU-145 cells that lack the expression of PSMA (data not shown). We are currently examining whether DβE can be employed for targeted delivery of liposomal drugs (including ODN) to PSMA-overexpressing prostate cancer cells. PSMA-mediated targeting might be advantageous over sigma receptor-based targeting since PSMA is more specific for prostrate cancer. Several studies have shown that PSMA is also overexpressed in what appears to be microvascular lining cells in prostate cancer and other tumors (Liu et al., 1997; Liu et al., 2002). Thus there might be a synergistic effect in PSMA-mediated targeting by killing both tumor cells and tumor endothelial cells.

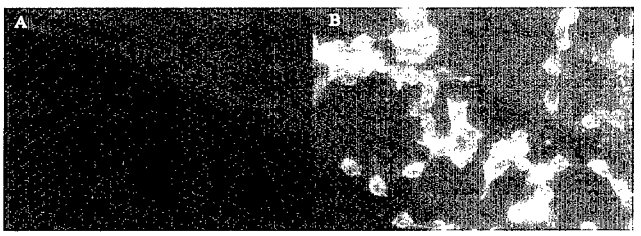

Fig. 2. DβE-mediated liposomal targeting to LNCaP cancer cells. *Rho-labeled liposomes composed of PC, cholesterol and PE-PEG with (B) or without (A) DSPE-PEG-DβE (0.5 mol%) were prepared and added to LNCaP cells. Liposomal uptake was examined one h later under a fluorescence microscope.*

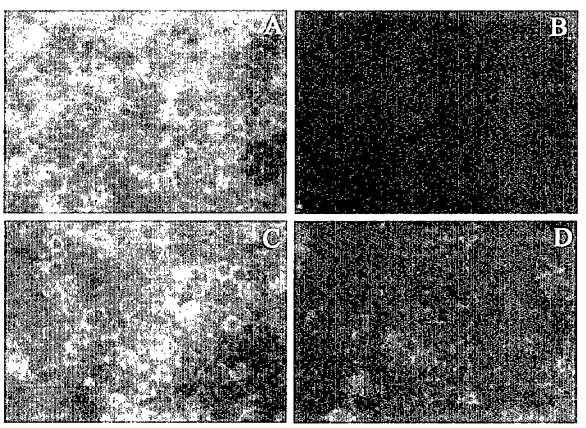

Fig. 3. EGFR expression in KB cells following targeted delivery of EGFR antisense ODN. *Cells were treated with ODN, free or formulated in FR-targeted lipid vesicles for 1 h and then cultured in normal medium. Expression of EGFR in KB cells 4 days following ODN treatment was then examined by an indirect immunofluorescent staining using mouse anti-human EGFR antibody. A: KB cells without treatment; B: negative control (cells reacted with blocking buffer followed by fluorescein-labeled goat anti-mouse IgG); C: KB cells treated with free EGFR antisense ODN; D: KB cells treated with antisense ODN formulated in FR-targeted lipid vesicles.*

2. Development of a novel lipid vector for targeted delivery of ODN: The major limitation with liposomal vectors for ODN delivery is the low encapsulation efficiency. A novel method has recently been reported to encapsulate ODN inside lipidic vesicles at a high efficiency (Semple et al., 2001). In this study, we were examining whether this vector can be modified to achieve targeted ODN delivery. This feasibility was examined using folate as a model ligand. A number of studies have shown that certain types of tumors overexpress folate receptors (FR). Folate has been used by our group and other groups to target anticancer agents to tumors that overexpress FR. Conventional FR-targeted liposomes suffer from a low entrapment efficiency for ODN delivery. We have successfully prepared FR-targeted lipidic ODN with ODN entrapment efficiency as high as 60-80% (w/w). The lipid composition is composed of DSPC: cholesterol: DODAP: DSPE-PEG: folate-PEG-PE. Folate mediates efficient targeting of ODN to KB cells that overexpress FR (Zhou et al., 2002). Targeted delivery of EGFR antisense ODN to KB cells led to a dramatic reduction in the EGFR expression as shown in an immuno-fluorescence assay (Figure 3), far more efficient than free antisense ODN. Down-regulation of EGFR expression via targeted antisense therapy greatly sensitizes KB cells to chemotherapy. Figure 4 shows the results of a MTT assay following treatment of KB cells with FR-targeted EGFR antisense ODN, doxorubicin (DOX), or a combination of both. Either antisense ODN or DOX exhibited only a low level of cytotoxic effect on KB cells. However, pretreatment with FR-targeted EGFR antisense ODN significantly enhances the cytotoxic effect of DOX on KB cells. We are currently extending this study to targeted delivery of ODN to prostate cancer via PSMA.

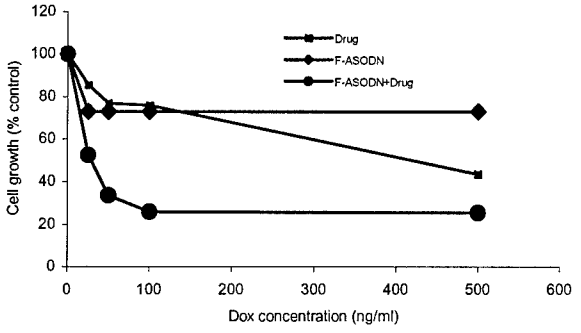

Fig. 4. Treatment with FR-targeted antisense ODN sensitizes KB cells to chemotherapy. *KB cells were treated with FR-targeted antisense ODN for 1 h and then cultured in normal medium. Two days later cells were exposed to various concentrations of DOX and cell growth was examined 1 day later by MTT assay.*

KEY RESEARCH ACCOMPLISHMENTS:

We have demonstrated for the first time that small molecular weight ligands including benzamide derivatives and DβE can be used to target liposomal drugs to prostate cancer cells in vitro and in vivo. The advantages of these targeting systems include: a) low immunogenecity; b) low toxicity due to the excellent safety profiles of benzamide and DβE. This strategy might be used to deliver to prostate cancer cells various types of anticancer agents including small molecular weight chemotherapeutic drugs, ODN and genes. Using folate as a model ligand, we have also developed a method to prepare

targeted lipidic ODN with a high ODN entrapment efficiency. The success of these studies will pave the way to our long-term goal of targeted delivery of Bcl-2 antisense ODN to prostate cancer.

REPORTABLE OUTCOMES:

Zhou, W., Yuan, X., Wilson, A., Yang, L., Mokotoff, M., Pitt, B., and **Li, S.** Efficient intracellular delivery of oligonucleotides formulated in folate receptor-targeted lipid vesicles. *Bioconjuagte Chemistry* 13: 1220-1225, 2002.

Yang, L., Zhou, W., and **Li, S.** Targeted delivery of antisense oligonucleotides to folate receptor-overexpressing tumor cells. *Journal of Controlled Release* 95: 321-331, 2004.

Banerjee R, Tyagi, P., **Li, S.**, and Huang, L. Anisamide-targeted stealth liposomes: a potent carrier for targeting doxorubicin to prostate cancer cells. *International Journal of Cancer* (in press) (*correspondence author).

CONCLUSIONS:

Sigma receptors or PSMA mediate efficient targeting of liposomal drugs to prostate cancer. Future studies will be planned to extend the above studies to targeting of Bcl-2 antisense oligonucleotides to prostate cancers.

REFERENCES:

Banerjee R, Tyagi, P., Li, S., and Huang, L. Anisamide-targeted stealth liposomes: a potent carrier for targeting doxorubicin to prostate cancer cells. *International Journal of Cancer* (in press)

Bauer JJ, Sesterhenn IA, Mostofi FK, McLeod DG, Srivastava S, Moul JW. Elevated levels of apoptosis regulator proteins p53 and bcl-2 are independent prognostic biomarkers in surgically treated clinically localized prostate cancer. J. Urol. 1996; 156: 1511-1516.

Berchem GJ, Bosseler M, Sugars LY, Voeller HJ, Zeitlin S, Gelmann EP. Androgens induce resistance to bcl-2-mediated apoptosis in LNCaP prostate cancer cells. Cancer Res. 1995; 55: 735-738.

Colombel M, Symmans F, Gil S, O'Toole KM, Chopin D, Benson M, Olsson CA, Korsmeyer S, Buttyan R. Detection of the apoptosis-suppressing oncoprotein bc1-2 in hormone-refractory human prostate cancers. Am. J. Pathol. 1993; 143: 390-400.

Denis L, Murphy GP. Overview of phase III trials on combined androgen treatment in patients with metastatic prostate cancer. Cancer 1993; 72: 3888-3895.

Ishida T, Kirchmeier MJ, Moase EH, Zalipsky S, Allen TM. Targeted delivery and triggered release of liposomal doxorubicin enhances cytotoxicity against human B lymphoma cells. Biochim Biophys Acta 2001 Dec 1;1515: 144-158.

John CS, Bowen WD, Saga T, Kinuya S, Vilner BJ, Baumgold J, Paik CH, Reba RC, Neumann RD, Varma VM, et al. A malignant melanoma imaging agent: synthesis, characterization, in vitro binding and biodistribution of iodine-125-(2-piperidinylaminoethyl)4-iodobenzamide. J. Nucl. Med. 1993; 34: 2169-2175.

John CS, Vilner BJ, Bowen WD. Synthesis and characterization of [125I]-N-(N-benzylpiperidin-4-yl)-4- iodobenzamide, a new sigma receptor radiopharmaceutical: high-affinity binding to MCF-7 breast tumor cells. J. Med. Chem.1994; 37: 1737-1739.

John CS, Vilner BJ, Gulden ME, Efange SM, Langason RB, Moody TW, Bowen WD. Synthesis and pharmacological characterization of 4-[125I]-N-(N-benzylpiperidin-4-yl)-4-iodobenzamide: a high affinity sigma receptor ligand for potential imaging of breast cancer. Cancer Res. 1995; 55: 3022-3027.

John CS, Vilner BJ, Geyer BC, Moody T, Bowen WD. Targeting sigma receptor-binding benzamides as in vivo diagnostic and therapeutic agents for human prostate tumors. Cancer Res. 1999a; 59: 4578-4583.

John CS, Bowen WD, Fisher SJ, Lim BB, Geyer BC, Vilner BJ, Wahl RL. Synthesis, in vitro pharmacologic characterization, and preclinical evaluation of N-[2-(1'-piperidinyl)ethyl]-3-[125I]iodo-4-methoxybenzamide (P[125I]MBA) for imaging breast cancer. Nucl. Med. Biol. 1999b; 26: 377-382.

Liu C, Huang H, Donate F, Dickinson C, Santucci R, El-Sheikh A, Vessella R, Edgington TS. Prostate-specific Membrane Antigen Directed Selective Thrombotic Infarction of Tumors. Cancer Res 2002 Oct 1;62(19):5470-5.

Liu H, Moy P, Kim S, Xia Y, Rajasekaran A, Navarro V, Knudsen B, Bander NH. Monoclonal antibodies to the extracellular domain of prostate-specific membrane antigen also react with tumor vascular endothelium. Cancer Res 1997 Sep 1;57(17):3629-34.

McConkey DJ, Greene G, Pettaway CA. Apoptosis resistance increases with metastatic potential in cells of the human LNCaP prostate carcinoma line. Cancer Res. 1996; 56:5594-5599.

McDonnell TJ, Troncoso P, Brisbay SM, Logothetis C, Chung LW, Hsieh JT, Tu SM, Campbell ML. Expression of the protooncogene bcl-2 in the prostate and its association with emergence of androgen-independent prostate cancer. Cancer Res. 1992; 52: 6940-6944.

Oh WK, Kantoff PW. Management of hormone refractory prostate cancer: current standards and future prospects. J. Urol. 1998; 160: 1220-1229.

Raffo AJ, Perlman H, Chen MW, Day ML, Streitman JS, Buttyan R. Overexpression of bcl-2 protects prostate cancer cells from apoptosis in vitro and confers resistance to androgen depletion in vivo. Cancer Res. 1995; 55: 4438-4445.

Semple SC, Klimuk SK, Harasym TO, Dos Santos N, Ansell SM, Wong KF, Maurer N, Stark H, Cullis PR, Hope MJ, Scherrer P. Efficient encapsulation of antisense oligonucleotides in lipid vesicles using ionizable aminolipids: formation of novel small multilamellar vesicle structures. Biochim. Biophys. Acta 2001; 1510: 152-166.

Vilner BJ, John CS, Bowen WD. Sigma-1 and sigma-2 receptors are expressed in a wide variety of human and rodent tumor cell lines. Cancer Res. 1995; 55: 408-413.
Zhou, W., Yuan, X., Wilson, A., Yang, L., Mokotoff, M., Pitt, B., and Li, S. Efficient intracellular delivery of oligonucleotides formulated in folate receptor-targeted lipid vesicles. *Bioconjuagte Chemistry* 13: 1220-1225, 2002.

Efficient Intracellular Delivery of Oligonucleotides Formulated in Folate Receptor-Targeted Lipid Vesicles

Wen Zhou,[†,‡] Xing Yuan,[†,‡] Annette Wilson,[§] Lijuan Yang,[†,‡] Michael Mokotoff,[‡] Bruce Pitt,[§] and Song Li*[,†,‡]

Center for Pharmacogenetics and Department of Pharmaceutical Sciences, School of Pharmacy; and Department of Environmental and Occupational Health, Graduate School of Public Health, University of Pittsburgh, Pittsburgh, Pennsylvania 15213. Received July 8, 2002; Revised Manuscript Received August 7, 2002

In this study, a novel lipid vector has been developed for targeted delivery of oligodeoxynucleotides (ODN) to tumors that overexpress folate receptor. This is based on a method developed by Semple et al. (*1*), which utilizes an ionizable aminolipid (1,2-dioleoyl-3-(dimethylammonio)propane, DODAP) and an ethanol-containing buffer system for encapsulating large quantities of polyanionic ODN in lipid vesicles. Folate is incorporated into the lipid vesicles via a distearoylphosphatidylethanolamine poly-(ethylene glycol) (DSPE PEG) spacer. These vesicles are around 100 200 nm in diameter with an ODN entrapment efficiency of 60 80%. Folate mediated efficient delivery of ODN to KB cells that overexpress folate receptor. Uptake of folate-targeted lipidic ODN by KB cells is about 8 10-fold more efficient than that of lipidic ODN without a ligand or free ODN. This formulation is resistant to serum. Thus, targeted delivery of ODN via this novel lipid vector may have potential in treating tumors that overexpress folate receptors.

INTRODUCTION

Functional oligodeoxynucleotides (ODN) such as antisense ODN and DNA enzymes hold promise as new therapeutics for the treatment of various types of diseases such as cancers (*2*, *3*). A number of studies have suggested the existence of ODN receptors on the cell surface (*4*, *5*). However, intracellular delivery of ODN without a delivery vehicle is generally inefficient. Successful application of therapeutic ODN is largely dependent on the development of a vehicle that selectively delivers the ODN into target cells with minimal toxicity. A number of vectors have been developed to improve the intracellular delivery of ODN such as neutral liposomes (*6*) and cationic liposomes (*7*, *8*). ODN can be entrapped inside neutral liposomes. The liposomes can also be designed such that they are long-circulating in the blood and target cell-specific. However, the size of liposomes required for achieving long circulation in the blood and efficient localization is too small for efficient entrapment of ODN. Cationic liposomes readily form complexes with ODN through electrostatic interactions. Almost 100% of ODN can be recovered in complex form. The resulting complexes usually contain slight excess amount of positive charges that allows efficient interaction with the negatively charged cell membrane. A number of cationic liposomes have been developed that significantly enhance the intracellular delivery of ODN. ODN complexed with cationic liposomes exhibit biological activity up to 1000-fold higher than ODN alone (*7*, *8*). However, targeted delivery of ODN to solid tumors via systemic administration remains problematic, although we have shown that cationic liposomes mediate efficient delivery of ODN to pulmonary endothelium (*9*). Recently, a novel lipid formulation has been developed (*1*) that appears to avoid the problems that are associated with each of the formulations discussed above. This formulation is composed of distearoylphosphatidylcholine (DSPC), cholesterol, DODAP, and *N*-palmitoylsphingosine-1-[succinyl-(methoxypoly(ethylene glycol))2000] (PEG-CerC_{16}). DODAP is an ionizable cationic lipid that has a pK of 6.6 in lipid bilayer systems. At acidic pH values (i.e. pH 4.0), this lipid is positively charged and helps to improve the ODN entrapment via electrostatic interactions. DODAP/ODN complexes can interact with other lipids in an ethanol-containing buffer, and ODN-containing lipid vesicles are formed upon the removal of the ethanol by dialysis. Subsequent adjustment of the external pH to neutral pH values results in a neutral surface charge on the resulting particles. This method led to a significant increase in ODN entrapment efficiency (60 80%) with a final lipid/ODN ratio of 0.15 0.25 (w/w) (*1*). This formulation has also been shown to be long circulating in the blood following systemic administration (*1*). In this study, we have shown that this formulation can be further improved via the incorporation of a targeting ligand, folate. Folate-targeted vesicles are much more efficient than the nontargeted vectors in delivering ODN to KB cells. This improved formulation may have potential for the targeted delivery of therapeutic oligonucleotides to tumors that overexpress folate receptors.

EXPERIMENTAL PROCEDURES

Lipids and Chemicals. Distearoylphosphatidylcholine (DSPC), *N*-palmitoylsphingosine-1-[succinyl(methoxypoly(ethylene glycol))2000] (PEG-CerC_{16}), and 1,2-dioleoyl-3-(dimethylammonio)propane (DODAP) were obtained from Avanti Polar Lipids, Inc. (Alabaster, AL). Folic acid

* Address correspondence to Dr. Song Li, Center for Pharmacogenetics, University of Pittsburgh School of Pharmacy, 639 Salk Hall, Pittsburgh, PA 15213, Tel: 412-383-7976, Fax: 412-648-1664, E-mail: sol4@pitt.edu.

† Center for Pharmacogenetics, School of Pharmacy.

‡ Department of Pharmaceutical Sciences, School of Pharmacy.

§ Department of Environmental and Occupational Health, Graduate School of Public Health.

10.1021/bc025569z CCC: $22.00
Published on Web 10/23/2002

Table 1. The Sequences of ODN Used in This Study

no.	sequence (5′-3′)
1	tat gat ctg tca cag ctt ga (*19*)
2	cgg agg gtc gca tcg ctg (*20*)
3	cac gcc ctt acc ttt ctt ttc ct (*20*)
4	ccg tgg tca tgc tcc (*6*)
5	ccc cag cag ctc cca ttg gg (*21*)
6	gct gac gca ctg act (*6*)

and cholesterol (CH) were purchased from Sigma-Aldrich. All lipids were 99% pure. Folate-free RPMI 1640 medium, F12 medium, and other tissue culture reagents were purchased from Gibco-BRL (Grand Island, NY). Folate poly(ethylene glycol) (MW ~ 3350 or 2000 Da) distearoyl phosphatidylethanolamine (folate PEG DSPE) was synthesized as described previously (10). The final folate PEG DSPE product was purified on a column of silica gel (70 200 mesh) using a solvent gradient of 15 to 80% methanol in CH_2Cl_2. Product purity was confirmed by thin-layer chromatography analysis on silica gel GF.

Antisense ODN. All ODN were synthesized with phosphorothioate (PS) backbone chemistry (the Midland Certified Reagent Company, Midland, TX). The sequences of ODN used in this study are shown in Table 1.

Preparation of ODN-Containing Lipid Vesicles. ODN-containing lipid vesicles were prepared according to the method described by Semple et al. (*1*) except that folate PEG DSPE was added when preparing the folate-targeted lipid vesicles. Briefly, a lipid solution composed of DSPC, cholesterol, DODAP, and PEG-CerC_{16} in 100% ethanol at indicated molar ratios (Figures 1 7) was prepared. For preparation of folate-targeted lipid vesicles, various amounts of folate PEG DSPE were added. To the lipid solution was then added 300 mM citric acid, pH 4.0 to a final ethanol concentration of 40% (v/v). Similarly, ODN were prepared in separate tubes in 300 mM citric acid, pH 4.0, with 40% ethanol. The solutions were prewarmed to 65 °C, and then the lipid solution was slowly added to the ODN with gentle vortexing. The input ratio was 150 μg ODN/μmol lipid. The mixture was passed 10 times through three stacked 100 nm polycarbonate filters. The preparation was dialyzed (12 14 kDa cutoff) against 300 mM citrate buffer, pH 4.0, for approximately 1 h to remove excess ethanol and further dialyzed against HBS (20 mM HEPES, 145 mM NaCl, pH 7.6) for 12 18 h to remove the citrate buffer, neutralize the DODAP, and release any ODN that was associated with the surface of the vesicles. ODN-containing lipid vesicles were finally separated from free ODN via gel filtration on a Sepharose CL-4B column (1 cm × 25 cm).

Cells and Medium. KB human cancer cells, derived from an epidermal carcinoma of the oral cavity, were obtained from American Type Culture Collection (ATCC). The cells were maintained in folate-free RPMI 1640 medium supplemented with 100 units/mL penicillin, 100 g/mL streptomycin, and 10% fetal bovine serum, which provides the only source of folate (the final folate concentration in the serum-supplemented medium was approximately physiological). The cells were cultured as a monolayer in a humidified atmosphere containing 5% CO_2 at 37 °C. CHO cells were obtained from ATCC and cultured in F12 medium supplemented with 10% fetal calf serum.

Uptake of ODN by KB and CHO Cells. Cells were seeded to a 24-well plate at a cell density of 2.5 × 10^4/well and allowed to grow overnight. ODN, free or encapsulated in lipid vesicles, were added to the cells in various concentrations [determined according to a carbocyanine dye (Cy3)-labeled ODN]. Following incubation at 37 °C for 1 h, cells were washed with PBS (3 × 3 min). Cells were lysed using a lysis buffer (0.1% Triton X in 100 mM Tris, 2 mM EDTA, pH 7.6). The lysed cells were centrifuged at 14000 rpm for 10 min at 4 °C. The amount of Cy3-labeled ODN in the supernatant was determined by examining its fluorescence intensity on a LS50B Perkin-Elmer Luminescence Spectrometer. The protein content of the supernatant was measured with Bio-Rad protein assay system (Bio-Rad, Hercules, CA). The result of ODN uptake was expressed as the pg Cy3-labeled ODN/μg protein.

Fluorescence Microscopic Examination of Cellular Uptake of Folate-Targeted Lipidic ODN. KB cells were seeded at a density of 1 × 10^5 cells/well in a 4-well Nalge Nunc Lab-Tek chamber slide (Naperville, IL) and kept overnight at 37 °C. ODN, free or formulated in lipid vesicles with or without a folate ligand, were added at a Cy3-ODN concentration of 100 ng/mL. In one well, free folate was added to the folate-targeted lipidic ODN at a final concentration of 1 mM. One hour following the incubation at 37 °C cells were washed three times with PBS. Cells were then fixed with 2% paraformaldehyde at 37 °C for 20 min and further washed three times with PBS. Cellular uptake of Cy3-labeled ODN was examined under a Nikon Eclipse TE 300 fluorescence microscope with a blue filter at 200× magnification.

RESULTS

Preparation and Characterization of Folate-Targeted, ODN-Containing Lipid Vesicles. Cy3-labeled ODN were used as a label for quantification of ODN encapsulation efficiency and for following the cellular uptake of ODN-containing lipid vesicles. Cy3-labeled ODN were mixed with unlabeled ODN at a 1:9 ratio (w/w). ODN were first mixed with a lipid solution composed of DSPC, cholesterol, DODAP, PEG-CerC_{16}, and folate PEG DSPE under an acidic condition in the presence of 40% ethanol. DODAP/ODN complexes and other lipids were then self-assembled to form ODN-containing lipid vesicles during the dialysis against 300 mM citrate buffer, pH 4.0, and then against HBS (20 mM HEPES, 145 mM NaCl, pH 7.6). Figure 1 shows the profile of separation of the mixture on Sepharose CL-4B. The lipid-associated ODN were well separated from free ODN. The size of the ODN-containing vesicles ranges from 100 to 200 nm with 60 80% of input ODN being associated with the lipid vectors. These vesicles carry a negative charge surface as confirmed by Zeta potential analysis (data not shown). The ODN that were associated with lipid vesicles were fully protected from degradation by nuclease, suggesting that ODN were encapsulated inside the lipid vesicles (data not shown). These studies were performed with six different ODN ranging from 15 to 23 mer in length (Table 1), and similar results were obtained.

Effect of the Amount of Folate PEG DSPE on the Cellular Uptake of Folate-Targeted Lipidic ODN. Figure 2 shows the cellular uptake of lipidic ODN by KB cells with increasing amount of input folate PEG DSPE. The total amount of lipid-derivatized PEG (folate PEG DSPE plus PEG-CerC_{16}) added is 2 mol %. Increasing the amount of folate from 0.1 to 0.5 mol % resulted in a significant increase in the cellular uptake of ODN. Increasing the input folate beyond 0.5 mol % was not associated with a further increase in the cellular uptake of ODN.

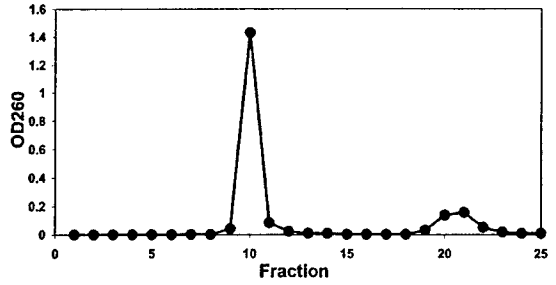

Figure 1. Size-exclusion chromatographic fractionation of ODN-containing lipid vesicles on a Sepharose CL-4B column. DSPC, cholesterol, DODAP, PEG-CerC_{16}, and folate PEG DSPE were individually dissolved in ethanol and mixed in a molar ratio of 25/45/25/4/1. To the lipid solution was added 300 mM citric acid, pH 4.0, to a final ethanol concentration of 40% (v/v). Similarly ODN were prepared in separate tubes in 300 mM citric acid, pH 4.0, with 40% ethanol. The solutions were prewarmed to 65 °C, and the lipids were slowly added to the ODN with gentle vortexing. The mixture was passed 10 times through three stacked 100 nm polycarbonate filters. The preparation was dialyzed (12 14 kDa cutoff) against 300 mM citrate buffer, pH 4.0, for approximately 1 h to remove excess ethanol and further dialyzed against HBS (20 mM HEPES, 145 mM NaCl, pH 7.6) for 12 18 h. The dialyzed solution (0.5 mL) was loaded on to a Sepharose CL-4B column (1 cm × 25 cm), which had been equilibrated with HEPES (pH7.6). Lipidic ODN and free ODN were collected with 1 mL in each fraction and examined for their absorbance at 260 nm.

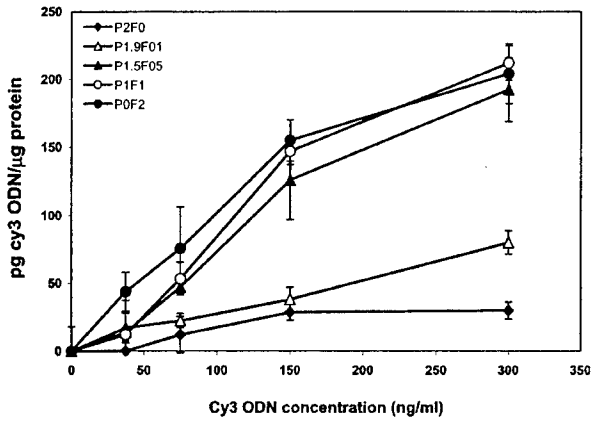

Figure 2. Effect of the amount of folate-PEG-DSPE on the cellular uptake of folate-targeted lipidic ODN. ODN-containing lipid vesicles were prepared as described in the legend to Figure 1 with various amounts of input folate PEG DSPE. The total amount of PEG added in the lipid mixture is 2 mol %. KB cells were seeded to a 24-well plate at a cell density of 2.5 × 10^4/well and allowed to grow overnight. Lipidic ODN were added to the cells in various concentrations (determined according to the Cy3-labeled ODN). Following incubation at 37 °C for 1 h, cells were washed with PBS and then lysed using a lysis buffer. The lysed cells were centrifuged at 14000*g* for 10 min at 4 °C. The amount of Cy3-labeled ODN in the supernatant was determined by examining its fluorescence intensity on a fluorometer. The protein content of the supernatant was measured with Bio-Rad protein assay system. The result of ODN uptake was expressed as the pg Cy3-labeled ODN/μg protein. The *x* and *y* in PxFy (Figures 2, 3, and 5) represent the mol % of PEG-Cer16 and folate PEG DSPE in the lipid vesicles, respectively. *n* 3.

Effect of the Amount of Ceramide-Derivatized PEG on the Cellular Uptake of Folate-Targeted Lipidic ODN. Figure 3 shows the effect of the amount of input ceramide-derivatized PEG on the cellular uptake of folate-targeted lipidic ODN. The amount of input folate PEG DSPE is 0.1 (Panel A) or 1 mol % (Panel B). Increasing the amount of ceramide-derivatized PEG from 0 to 10 mol % resulted in a significant decrease in

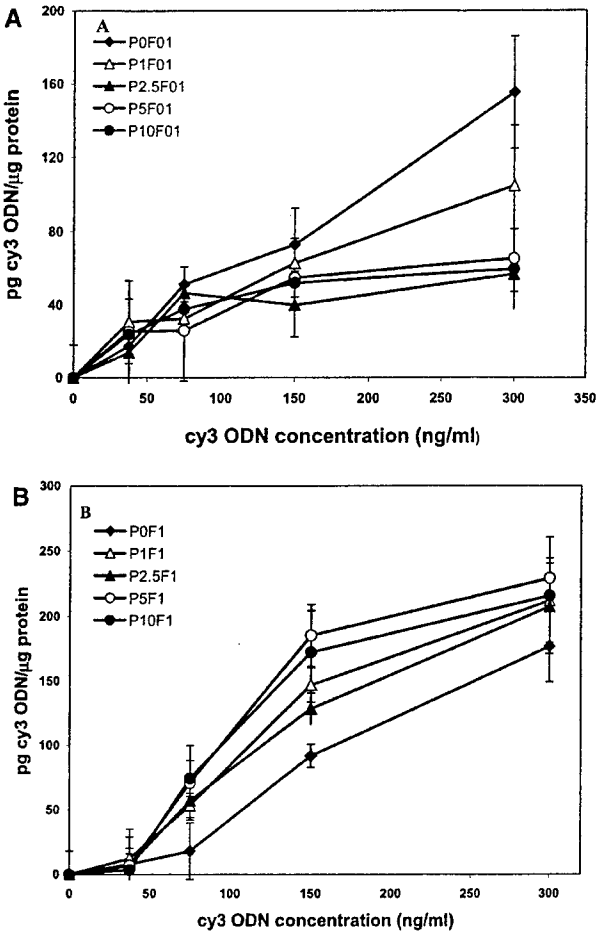

Figure 3. Effect of the amount of ceramide-PEG on the cellular uptake of folate-targeted lipidic ODN. ODN-containing lipid vesicles were prepared as described in the legend to Figure 1 with various amounts of input ceramide-PEG. The amount of input folate PEG DSPE was 0.1 mol % (Panel A) or 1 mol % (Panel B). Various amounts of ODN were added to KB cells and the cellular uptake of ODN was evaluated as described in the legend to Figure 2. *n* 3.

the cellular uptake of ODN when 0.1 mol % of folate PEG DSPE was used (Panel A). However, such an inhibitory effect was diminished when the amount of input folate PEG DSPE was increased to 1 mol % (Panel B).

Effect of PEG Length on the Cellular Uptake of Lipidic ODN. Previous studies have shown that folate-mediated targeting of liposomes is affected by the length of PEG spacer between folate and the lipid anchor (such as DSPE in this study) (*10, 11*). Similar results were observed in this study with ODN targeting using our new lipidic vector (Figure 4). Folate with a PEG of 3500 Da appeared to be more efficient than that with a PEG of 2000 Da in mediating the targeting of ODN to KB cells. This difference became more dramatic with increasing amounts of ceramide PEG (data not shown).

Cellular Uptake of Folate-Conjugated, Lipidic ODN is Mediated by Folate Receptors. To demonstrate whether the cellular uptake of folate-conjugated, lipidic ODN is mediated by folate receptor, their uptake was also examined on CHO cells, which have a low level of folate receptors (Figure 5). As shown in Panel A, coupling of folate to lipidic ODN led to a significant increase in the cellular uptake by KB cells. The level of ODN uptake was about 8 10-fold higher for folate-

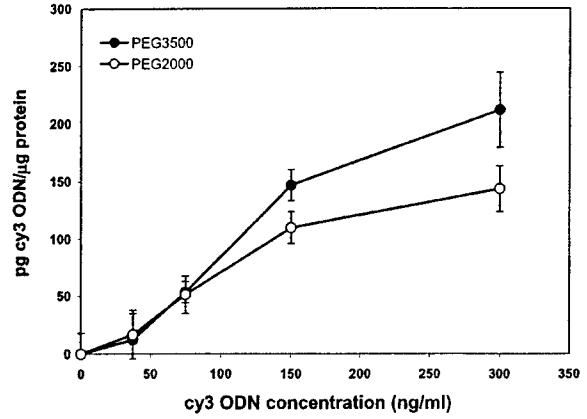

Figure 4. Effect of PEG length on the cellular uptake of lipidic ODN. Lipidic ODN were prepared as described in the legend to Figure 1. The molecular weight of PEG in folate PEG DSPE was 2000 or 3500 Da. Various amounts of ODN were added to KB cells and the cellular uptake of ODN was evaluated as described in the legend to Figure 2. *n* 3.

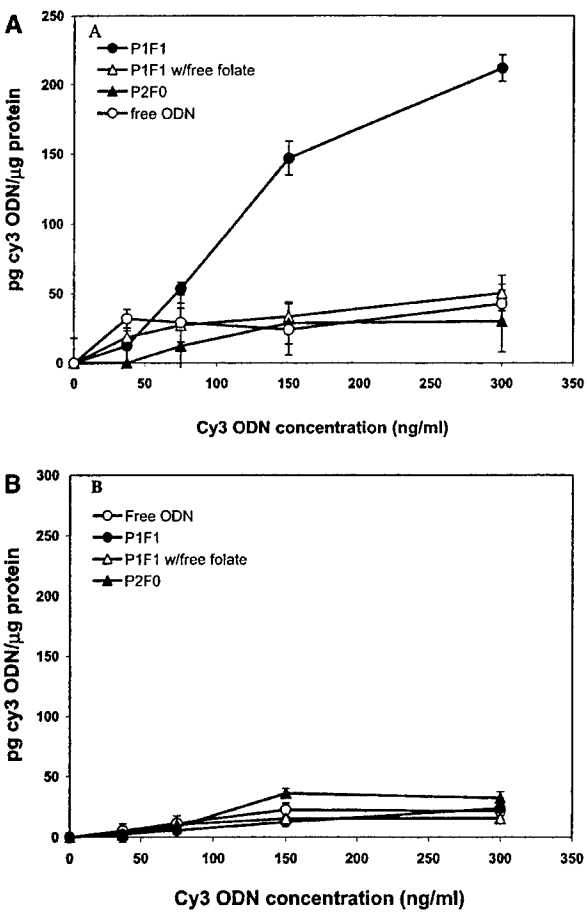

Figure 5. Cell type-specific uptake of folate-targeted lipidic ODN. KB (Panel A) or CHO (Panel B) cells were plated in a 24-well plate. ODN, free or formulated in lipid vesicles with or without a folate ligand, were added to cells in various concentrations. In a separate experiment, free folate was added to folate-targeted lipidic ODN at a final concentration of 1 mM. Cellular uptake of ODN was then evaluated as described in the legend to Figure 2. *n* 3.

targeted lipidic ODN than that of free ODN or lipidic ODN without a ligand. The improvement in ODN uptake was almost completely blocked by adding excess amount of free folate. There was essentially no difference in the ODN uptake by CHO cells whether ODN were free or formulated in ligand-free lipid vesicles or folate-targeted lipid vesicles (Panel B).

Fluorescence Microscopic Examination of the Cellular Uptake of Folate-Targeted Lipidic ODN. Figure 6 shows the fluorescence images of ODN uptake by KB cells. At 1 h following incubation at 37 °C, folate-targeted ODN were found to be associated with the cell membrane as well as inside the cells (Panel B). In agreement with the quantitative analysis (Figure 5), the level of cell-associated fluorescence intensity is substantially higher with folate-targeted ODN (Panel B) than that with either free ODN (Panel D) or ODN formulated in nontargeted lipid vesicles (Panel A). However, the fluorescence intensity with folate-targeted ODN was decreased to background level by adding excess amounts of free folate (Panel C). These results suggest that the binding and the subsequent internalization of the folate-targeted ODN are mediated by the folate receptors.

Effect of Serum on ODN Uptake by KB Cells. Figure 7 shows the uptake of folate-targeted ODN by KB cells in the presence or absence of 10% FBS. Serum appears to have only a slight effect on the cellular uptake of folate-targeted ODN. Similar phenomenon was observed for free ODN or ODN formulated in nontargeted lipid vesicles (data not shown).

DISCUSSION

An ideal ODN vector should have a large ODN loading capacity and deliver the ODN to target cells in a cell-type-specific manner. Neutral liposomes are suitable for active targeting but suffer from low encapsulation efficiencies and drug-to-lipid ratios. This problem can be resolved via incorporation of cationic lipids into the formulation, but the resulting lipid/nucleic acid complexes are generally unstable and short-lived in blood circulation. Furthermore, substantial amounts of ODN are associated with the positively charged surface of the particles. These ODN may be released from the particles by the highly negatively charged molecules in the blood following systemic administration (*12*). Recently, Stuart and Allen (*13*) described a method by which 80 100% of input ODN were entrapped in a lipid vector that was stable in human plasma. This involves the formation in and extraction of cationic lipid/ODN complex from an organic solvent. The cationic lipid/ODN complex was then mixed with other neutral lipids and ODN-containing lipid vesicles were obtained by a reverse phase evaporation method (*13*). More recently, a much simpler method was developed by Semple and colleagues (*1*), which utilizes an ionizable aminolipid (DODAP) and an ethanol-containing buffer system. A similar level of encapsulation efficiency was achieved (*1*). These ODN-containing lipid vesicles, however, are inefficient in interacting with cells. Furthermore, they lack cell type specificity. In this study we investigated whether a targeting ligand can be incorporated into these vesicles to further improve their efficiency in intracellular delivery of ODN. Folate was chosen as a targeting ligand since folate receptors have been shown to be overexpressed in a number of cancer cells. Folate has been used successfully in targeting to tumors various types of agents including chemotherapeutic drugs (*10*), radionucleotides (*14, 15*), ODN (*6, 16*), DNA (*17, 18*), etc. The advantages of a folate-targeting system include its excellent safety profile and the low immunogenicity. Folate receptors have also been shown to mediate efficient internalization of free folate or the

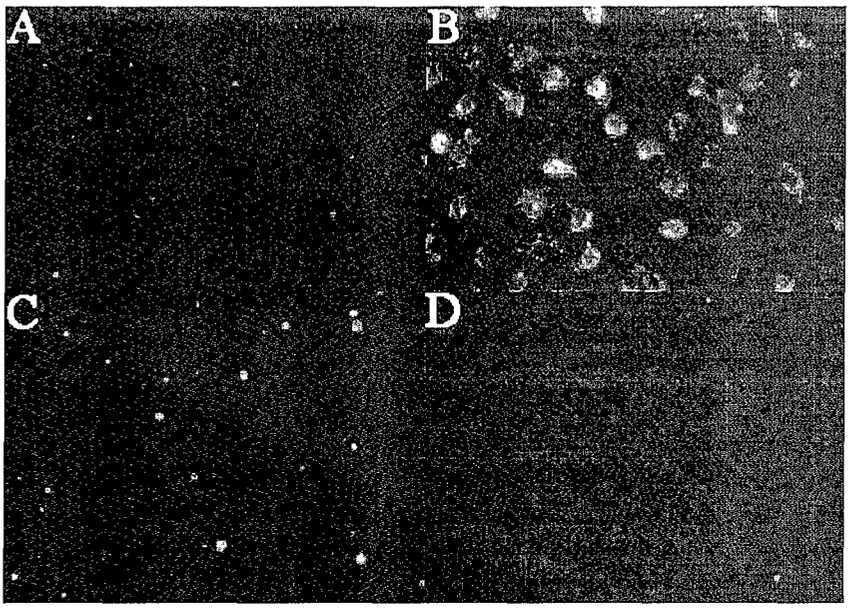

Figure 6. Fluorescence microscopic examination of cellular uptake of folate-targeted lipidic ODN. KB cells were seeded at a density of 1×10^5 cells/well in a 4-well Nalge Nunc Lab-Tek chamber slide (Naperville, IL) and kept overnight at 37 °C. ODN, free or formulated in lipid vesicles with or without a folate ligand, were added at a Cy3-ODN concentration of 100 ng/mL. In one well, free folate was added to the folate-targeted lipidic ODN at a final concentration of 1 mM. One hour following the incubation at 37 °C cells were washed three times with PBS. Cells were then fixed with 2% paraformaldehyde at 37 °C for 20 min and further washed with PBS three times. Cellular uptake of Cy3-labeled ODN was examined under a Nikon fluorescence microscope with a blue filter at 200X magnification. A: Lipidic ODN without a ligand; B: folate-targeted lipidic ODN; C: folate-targeted lipidic ODN + 1 mM free folate; D: free ODN.

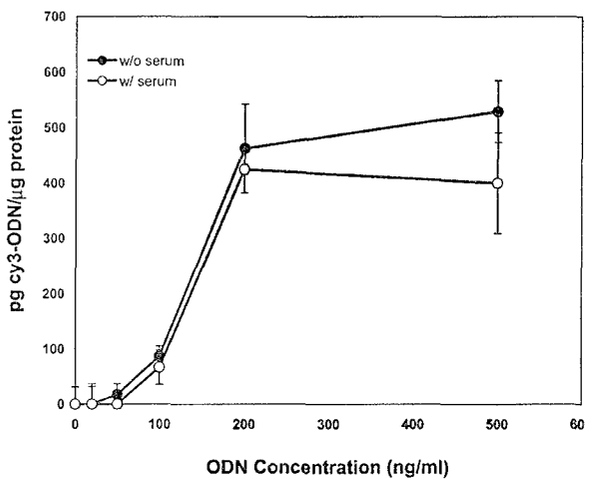

Figure 7. Effect of serum on ODN uptake by KB cells. KB cells were seeded to a 24-well plate at a cell density of 2.5×10^4/well and allowed to grow overnight. Various concentrations of folate-targeted ODN were added to cells in the presence or absence of 10% FBS. Cellular uptake of ODN was then evaluated as described in the legend to Figure 2. $n = 3$.

conjugates, which should facilitate intracellular delivery of the therapeutic agent. Results from this study clearly show that incorporation of folate into the ODN-containing vesicles leads to a significant improvement in delivery of ODN to KB cells that overexpress folate receptors (Figures 5 and 6). The increase in the ODN uptake was almost completely blocked by excess amount of free folate (Figures 5 and 6). Conjugation of folate led to little change in ODN uptake by CHO cells that are negative for folate receptor expression (Figure 5). These studies clearly indicate that targeted delivery of ODN to KB cells via this novel lipid vector is mediated by the folate receptors.

The targeting efficiency of folate-conjugated vesicles is affected by the amount of input folate–PEG–DSPE. Increasing the amount of folate from 0 to 0.5 mol % was associated with a significant increase in ODN uptake. However, increasing the input folate beyond 0.5 mol % was not associated with a further increase in the cellular uptake of ODN (Figure 2). Interestingly, the targeting efficiency of folate-conjugated vesicles is also affected by the amount of input ceramide–PEG (Figure 3). Ceramide–PEG was included for two purposes: (a) to render the resulting particles long-circulating in the blood, and (b) to prevent aggregation during the preparation of ODN-containing lipid vesicles, particularly when the vectors were prepared at high lipid concentrations. However, at a high concentration of ceramide-PEG, substantial amounts of PEG have been shown to be excluded from the lipid vesicles (*1*). Similarly, some of the input folate might be excluded from the vesicles, which may lead to incoporation of less than sufficient amounts of folate needed to achieve efficient targeting when a small amount of input folate–PEG–DSPE is used. This may explain the fact that, at a folate concentration of 0.1 mol %, the efficiency of ODN delivery was decreased dramatically when the ceramide–PEG was increased to above 2.5 mol % (Figure 3A). This problem, however, can be resolved by increasing the amount of input folate–PEG–DSPE. As shown in Figure 3B, increasing the amount of input folate from 0.1 to 1 mol % resulted in a full recovery of targeting efficiency at high concentrations of ceramide–PEG (above 5 mol %). No purification is required to remove the free folate–PEG–DSPE from the folate-conjugated, ODN-containing lipid vesicles.

Similar to liposomal targeting (*10*, *11*), the efficiency of ODN delivery via the new lipid vector is affected by the length of the PEG spacer. This might be due to the fact that the PEG coating imposes steric hindrance for

the folate to interact efficiently with the folate receptors on the cell surface when a short PEG spacer (such as 2000 Da) is used. This interference becomes more pronounced with increasing amounts of ceramide PEG (data not shown). This problem, however, can be resolved via the use of a longer PEG spacer between the folate and the lipid anchor. As shown in Figure 4, increasing the length of PEG spacer from 2000 to 3500 Da results in a significant improvement in the targeting efficiency. Furthermore, the targeting efficiency of the resulting lipid vectors is not significantly affected by the amount of the input ceramide PEG (Figure 3B).

In summary, we have developed a novel lipid vector that is highly efficient in delivering ODN to tumor cells that overexpress folate receptor. We have also shown recently that this vector mediates efficient delivery of ODN to mouse lung endothelial cells using an endothelial cell-specific antibody as a ligand (Wilson et al., unpublished data). Currently we are examining the targeting efficiency of this vector in vivo.

ACKNOWLEDGMENT

This work was supported by DOD grant PC001525 and NIH grant HL RO1 63080 (to S Li). We would like to thank Dr. Takuro Niidome for his helpful discussion in this study.

LITERATURE CITED

(1) Semple, S. C., Klimuk, S. K., Harasym, T. O., Dos Santos, N., Ansell, S. M., Wong, K. F., Maurer, N., Stark, H., Cullis, P. R., Hope, M. J., and Scherrer, P. (2001) Efficient encapsulation of antisense oligonucleotides in lipid vesicles using ionizable aminolipids: formation of novel small multilamellar vesicle structures. *Biochim. Biophys. Acta 1510* (1 2), 152 66.

(2) Agrawal, S., and Zhao, Q. (1998) Antisense therapeutics. *Curr. Opin. Chem. Biol. 2* (4), 519 528.

(3) Crooke, S. T. (1998) An overview of progress in antisense therapeutics. *Antisense Nucleic Acid Drug Dev. 8* (2), 115 122.

(4) Yakubov, L. A., Deeva, E. A., Zarytova, V. F., Ivanova, E. M., Ryte, A. S., Yurchenko, L. V., and Vlassov, V. V. (1989) Mechanism of oligonucleotide uptake by cells: involvement of specific receptors? *Proc. Natl. Acad. Sci. U.S.A. 86* (17), 6454 6458.

(5) Loke, S. L., Stein, C. A., Zhang, X. H., Mori, K., Nakanishi, M., Subasinghe, C., Cohen, J. S., and Neckers LM. (1989) Characterization of oligonucleotide transport into living cells. *Proc. Natl. Acad. Sci. U.S.A. 86* (10), 3474 3478.

(6) Wang, S., Lee, R. J., Cauchon, G., Gorenstein, D. G., and Low, P. S. (1995) Delivery of antisense oligodeoxyribonucleotides against the human epidermal growth factor receptor into cultured KB cells with liposomes conjugated to folate via poly(ethylene glycol). *Proc. Natl. Acad. Sci. U.S.A. 92* (8), 3318 3322.

(7) Bennett, C. F., Chiang, M. Y., Chan, H., Shoemaker, J. E., and Mirabelli, C. K. (1992) Cationic lipids enhance cellular uptake and activity of phosphorothioate antisense oligonucleotides. *Mol. Pharmacol. 41*(6), 1023 1033.

(8) Cumin, F., Asselbergs, F., Lartigot, M., and Felder, E. (1993) Modulation of human prorenin gene expression by antisense oligonucleotides in transfected CHO cells. *Eur. J. Biochem. 212* (2), 347 354.

(9) Ma, Z., Zhang, J., Alber, S., Dileo, J., Negishi, Y., Stolz, D., Watkins, S. C., Huang, L., Pitt, B., and Li S. (2002) Lipid-mediated delivery of oligonucleotide to pulmonary endothelium. *Am. J. Respir. Cell Mol. Biol. 27* (2), 151 159.

(10) Lee, R. J., and Low, P. S. (1995) Folate-mediated tumor cell targeting of liposome-entrapped doxorubicin in vitro. *Biochim. Biophys. Acta 1233* (2), 134 44.

(11) Gabizon, A., Horowitz, A. T., Goren, D., Tzemach, D., Mandelbaum-Shavit, F., Qazen, M. M., and Zalipsky S. (1999) Targeting folate receptor with folate linked to extremities of poly(ethylene glycol)-grafted liposomes: in vitro studies. *Bioconjugate Chem. 10* (2), 289 298.

(12) Zelphati, O., and Szoka, F. C., Jr. (1996) Mechanism of oligonucleotide release from cationic liposomes. *Proc. Natl. Acad. Sci. U.S.A. 93* (21), 11493 11498.

(13) Stuart, D. D., and Allen, T. M. (2000) A new liposomal formulation for antisense oligodeoxynucleotides with small size, high incorporation efficiency and good stability. *Biochim. Biophys. Acta 463* (2), 219 29.

(14) Mathias, C. J., Wang, S., Lee, R. J., Waters, D. J., Low, P. S., and Green, M. A. (1996) Tumor-selective radiopharmaceutical targeting via receptor-mediated endocytosis of gallium-67-deferoxamine-folate. *J. Nucl. Med. 37*(6), 1003 1008.

(15) Guo, W., Hinkle, G. H., and Lee, R. J. (1999) 99mTc HYNIC-folate: a novel receptor-based targeted radiopharmaceutical for tumor imaging. *J. Nucl. Med. 40* (9), 1563 1569.

(16) Li, S., Deshmukh, H. M., and Huang, L. (1998) Folate-mediated targeting of antisense oligodeoxynucleotides to ovarian cancer cells. *Pharm. Res. 15* (10), 1540 1545.

(17) Lee, R. J., and Huang, L. (1996) Folate-targeted, anionic liposome-entrapped polylysine-condensed DNA for tumor cell-specific gene transfer. *J. Biol. Chem. 271* (14), 8481 8487.

(18) Xu, L., Pirollo, K. F., and Chang, E. H. (2001) Tumor-targeted p53-gene therapy enhances the efficacy of conventional chemo/radiotherapy. *J. Controlled Release 74* (1 3), 115 128.

(19) Ciardiello F., Caputo, R., Troiani, T., Borriello, G., Kandimalla, E. R., Agrawal, S., Mendelsohn, J., Bianco, A. R., and Tortora, G. (2001) Antisense oligonucleotides targeting the epidermal growth factor receptor inhibit proliferation, induce apoptosis, and cooperate with cytotoxic drugs in human cancer cell lines. *Int. J.* Cancer *93* (2), 172 178.

(20) Grandis, J. R., Chakraborty, A., Melhem, M. F., Zeng, Q., and Tweardy, D. J. (1997) Inhibition of epidermal growth factor receptor gene expression and function decreases proliferation of head and neck squamous carcinoma but not normal mucosal epithelial cells. *Oncogene 15*, 409 416.

(21) Witters, L., Kumar, R., Mandal, M., Bennett, C. F., Miraglia, L., and Lipton, A. (1999) Antisense oligonucleotides to the epidermal growth factor receptor. *Breast Cancer Res. Treat. 53*, 41 50.

BC025569Z

Available online at www.sciencedirect.com
SCIENCE DIRECT
Journal of Controlled Release 95 (2004) 321–331
journal of controlled release
www.elsevier.com/locate/jconrel

Targeted delivery of antisense oligodeoxynucleotides to folate receptor-overexpressing tumor cells

Lijuan Yang, Jiang Li, Wen Zhou, Xing Yuan, Song Li*

Center for Pharmacogenetics, Department of Pharmaceutical Sciences, School of Pharmacy, University of Pittsburgh, 639 Salk Hall, Pittsburgh, PA 15213, USA

Received 28 July 2003; accepted 30 November 2003

Abstract

A major problem in exploring the full potential of antisense ODN is the lack of a safe and efficient delivery system. In this study a new method has been developed that is highly efficient in encapsulating ODN inside folate receptor (FR)-targeted lipid vesicles. ODN formulated in these vesicles were efficiently protected from degradation by nucleases compared to free ODN. Folate efficiently mediated intracellular delivery of ODN to KB tumor cells that overexpress FR. Delivery of EGFR antisense ODN via FR-targeted lipid vesicles resulted in a significant down-regulation of EGFR expression in KB cells and cell growth inhibition, far more efficient than that with free ODN or ODN encapsulated in ligand-free lipid vesicles. Intracellular delivery of EGFR antisense ODN also sensitized KB cells to doxorubicin (DOX) treatment. Thus targeted delivery of ODN via this novel lipid vector may have potential in treating tumors that overexpress FR.

Keywords: Antisense; Oligodeoxynucleotides; Folate; Targeting; Lipid vector

1. Introduction

Antisense ODN are short sequence specific single stranded DNA molecules designed to bind to the mRNA of the target protein and show promise as a new type of anticancer therapeutics [1,2]. Their successful application is largely dependent, among others, on the development of a specific delivery vehicle. A number of vectors have been developed to improve their cellular uptake such as cationic liposomes [3,4] and neutral liposomes [5]. Cationic liposomes can readily form complexes with ODN through charge interaction and almost 100% of the ODN can be recovered in complexed form [3,4]. The resulting cationic liposome/ODN complexes usually carry slight excess positive charge, which allows efficient interaction with the negatively charged cell membrane [3,4]. However, due to the non-discriminative nature of cationic liposome/DNA complexes in interacting with cells, targeted delivery of ODN to tumor cells via systemic route remains problematic [6,7]. Neutral or anionic liposomes poorly interact with cells and a targeting ligand can be incorporated to achieve cell-type-specific delivery [5,8]. These formulations, however, suffer from low encapsulation efficiency due to

* Corresponding author. Tel.: +1-412-383-7976; fax: +1-412-648-1664.
E-mail address: sol4@pitt.edu (S. Li).

0168-3659/$ - see front matter © 2004 Elsevier B.V. All rights reserved.
doi:10.1016/j.jconrel.2003.11.021

the limited interior size of liposomes and the poor interaction of ODN with neutral or anionic lipids. Cullis and colleagues [9] have described a novel lipid formulation that appears to overcome this problem. This involves the use of an ionizable cationic lipid that has a pK_a around 6.5. At low pH values (e.g. 4.5) it is positively charged and thus efficiently interacts with ODN [9]. The resulting cationic lipid/ODN complex can be co-solubilized with other neutral lipids in a citric buffer containing 40% of ethanol. Subsequent removal of ethanol by dialysis results in the formation of ODN-containing lipid vesicles via a self-assembling process. The positive charge of the vesicles is then neutralized by further dialysis against a HEPES buffer of pH 7.6 [9]. As high as 60–80% of the input ODN was encapsulated in the lipid vesicles with a final ODN/lipid ratio of 0.15–0.25 (w/w) [9]. These ODN-containing lipid vesicles were shown to be long-circulating in blood following intravenous injection [9]. It has been recently demonstrated that this formulation can be further improved via inclusion of a targeting ligand [10]. Incorporation of a folate ligand led to a dramatic improvement in delivery of ODN to KB cells that overexpress folate receptors (FR) [10]. In this study, this formulation is further characterized with respect to its sensitivity to degradation by nucleases and the intracellular trafficking. Its potential in delivering EGFR antisense ODN to KB cells was also studied.

2. Materials and methods

2.1. Lipids and chemicals

Distearoylphosphatidylcholine (DSPC), 1,2-dioleoyl-3-dimethylammonium propane (DODAP), and *N*-palmitoyl-sphingosine-1-[succinyl (methoxypolyethylene glycol) 2000] (PEG-CerC16) were obtained from Avanti Polar Lipids (Alabaster, AL). Folic acid, doxorubicin (DOX), and cholesterol (CH) were purchased from Sigma-Aldrich (St. Louis, MO). All lipids were >99% pure. Folate-free RPMI 1640 medium and other tissue culture reagents were purchased from Gibco-BRL (Grand Island, NY). Distearoyl phosphatidylethanolamine–PEG–folate (DSPE–PEG–folate) was synthesized as described previously [10].

2.2. Antisense ODN

All ODN were synthesized with phosphorothioate (PS) backbone chemistry (The Midland Certified Reagent Company, Midland, TX). Some ODN were synthesized with a 5′-Cy3 label for confocal studies. The first antisense ODN (5′-TATGATCTGTCACAGCTTGA-3′) [sODN (1)] was directed against nucleotides 2457–2476 of the human EGFR mRNA [11]. The second antisense ODN (5′-CGGAGGGTCGCATCGCTG-3′) [sODN (2)] was directed against the translation start site and surrounding nucleotides of the human EGFR gene [12]. The sequence of control ODN is 5′-TCGCACCCATCTCTCTCCTTC-3′ [11].

2.3. Preparation of FR-targeted ODN-containing vesicles

FR-targeted lipidic ODN were prepared as described previously [10]. Briefly, a lipid solution composed of DSPC, CH, DODAP, and PEG-CerC16 (25/45/20/10, m/m) in 100% ethanol was prepared. For preparation of FR-targeted lipid vesicles 1 mol% of DSPE–PEG–folate was added. To the lipid solution was then added 300 mM citric acid, pH 4.0 to a final ethanol concentration of 40% (v/v). Similarly, ODN were prepared in separate tubes in 300 mM citric acid, pH 4.0 with 40% ethanol. The solutions were pre-warmed to 65 °C and then the lipid solution was slowly added to the ODN with gentle vortexing. The input ratio was 150 μg ODN per μmol lipid. The mixture was passed 10 times through three stacked 100 nm polycarbonate filters. The preparation was dialyzed (12–14 kDa cutoff) against 300 mM citrate buffer, pH 4.0 for approximately 1 h to remove excess ethanol and further dialyzed against HBS (20 mM HEPES, 145 mM NaCl, pH 7.6) for 12–18 h to remove the citrate buffer, neutralize the DODAP and release any ODN that were associated with the surface of the vesicles. ODN-containing lipid vesicles were finally separated from free ODN via gel filtration on a Sepharose CL-4B column (1 cm × 25 cm).

2.4. Cell culture and medium

KB human cancer cells, derived from an epidermal carcinoma of the oral cavity, were obtained from American Type Culture Collection (ATCC, Rockville, MD). The cells were maintained in folate-free RPMI 1640 medium supplemented with streptomycin (100 μg/ml) and penicillin (100 U/ml), and 10% fetal bovine serum, which provides the only source of folate (the final folate concentration in the serum-supplemented medium was approximately physiological). The cells were cultured as a monolayer in a humidified atmosphere containing 5% CO_2 at 37 °C.

2.5. Nuclease protection assays

Phosphodiester (PO) ODN, free or formulated in FR-targeted lipid vesicles, were incubated at 37 °C with excess S1 nuclease (100 U nuclease per μg ODN). At various times, aliquots were removed, placed in proteinase K buffer (10 mM Tris, pH 8.0, 100 mM NaCl, 25 mM EDTA, 0.5% SDS and 1 mg/ml proteinase K) and incubated at 50 °C for 1 h. Samples were added to an equal volume of stop buffer (93.6% formamide, 20 mM EDTA, 0.05% bromophenol blue) and analyzed on a denaturing 20% PAGE gel containing 7 M urea.

2.6. Intracellular delivery of ODN to KB cells via the FR-targeted lipid vesicles

KB cells were seeded at a density of 5×10^3 cells per well in a 8-well Nalge Nunc Lab-Tek chamber slide (Naperville, IL) and kept overnight at 37 °C. sODN, free or formulated in lipid vesicles with or without a folate ligand, were added at a Cy3-sODN concentration of 200 ng/ml and incubated at 37 °C for various times (5 and 15 min and 1 h). Cells were washed with PBS three times and fixed with 2% paraformaldehyde at 4 °C for 20 min and further washed three times with PBS. Cells were permeabilized with Triton X-100 (0.2% v/v in PBS) for 10 min at RT. After another three washes with PBS cells were stained with SYTOX Green to label the nucleus and then observed under a Leica TCS NT confocal microscope with a 60× oil immersion objective at a 1024 × 1024 pixel resolution.

2.7. Immunofluorescence analysis of EGFR expression in KB cells following targeted delivery of EGFR antisense ODN

KB cells were treated for 1 h with antisense sODN (free or formulated in FR-targeted lipid vesicles) at a concentration of 3 μM (folate concentration around 0.1 μM) and then cultured in normal medium for 4 days. Cells were fixed in 2% paraformaldehyde at 4 °C for 20 min. After three washes with PBS cells were incubated in blocking buffer (0.2% normal goat serum in PBS) at 4 °C for 1 h. Cells were then labeled with mouse anti-human EGFR monoclonal antibody (20 μg/ml in blocking buffer, Santa Cruz Biotechnology, Santa Cruz, CA) for 1 h at RT. Cells were washed with PBS three times and then reacted with fluorescein-labeled goat anti-mouse IgG (10 μg/ml, Santa Cruz Biotechnology) for 1 h at RT. After another three washes with PBS cells were examined under a fluorescence microscope.

2.8. Western blotting

KB cells were treated for 1 h with antisense sODN (free or formulated in FR-targeted lipid vesicles) at a concentration of 3 μM and then cultured in normal medium for 4 days. Cells were scraped and analyzed by Western blotting as described [13]. Mouse anti-human EGFR IgG was purchased from Upstate Biotechnology (Lake Placid, NY, USA). Horseradish peroxidase-conjugated anti-mouse secondary antibody was purchased from Promega (Madison, WI, USA).

2.9. Effect of antisense ODN treatment on the growth of KB cells

Cytotoxicity was evaluated by both trypan blue dye exclusion assay and MTT colorimetric assay. For the former assay, KB cells were seeded to a 24-well plate at a cell density of 2×10^4 per well and allowed to grow overnight. sODN, free or formulated in FR-targeted lipid vesicles, were added to the cells at a final concentration of 3 μM. Following incubation at 37 °C for 1 h, cells were washed with PBS twice and then continued to culture in normal medium and the cell numbers were counted at days 2, 4 and 6.

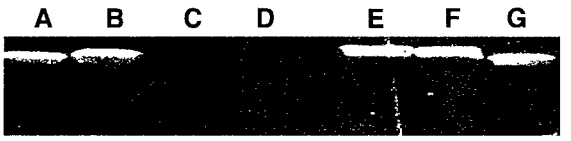

Fig. 1. Nuclease protection assays. ODN, free or formulated in FR-targeted lipid vesicles were incubated with or without S1 nuclease in digestion buffer at 37 °C for 5 or 30 min and were then examined for their integrity on PAGE gel. A and G, free ODN; B, free ODN incubated in digestion buffer without S1 nuclease for 30 min; C, free ODN incubated with S1 nuclease for 5 min; D, free ODN incubated with S1 nuclease for 30 min; E, lipidic ODN incubated with S1 nuclease for 30 min; F, lipidic ODN incubated in digestion buffer without S1 nuclease for 30 min.

For MTT colorimetric assay KB cells were seeded to a 96-well plate at a cell density of 0.5×10^3 per well and allowed to grow overnight. Cells then received sODN treatment as described above. Cytotoxicity at day 4 was examined by MTT assay as described previously [14].

For repeated dosing experiment KB cells were seeded to a 24-well plate at a cell density of 2×10^4 per well and allowed to grow overnight. Cells received sODN treatment as described above twice at days 0 and 3, and the cell numbers were counted at day 7.

2.10. Effect of combined treatment of targeted antisense therapy and chemotherapy on KB cells

KB cells were seeded to a 96-well plate and exposed to FR-targeted lipidic sODN at an ODN concentration of 0.3 or 1.5 μM. Two days later cells were exposed to DOX at a concentration of 50 ng/ml.

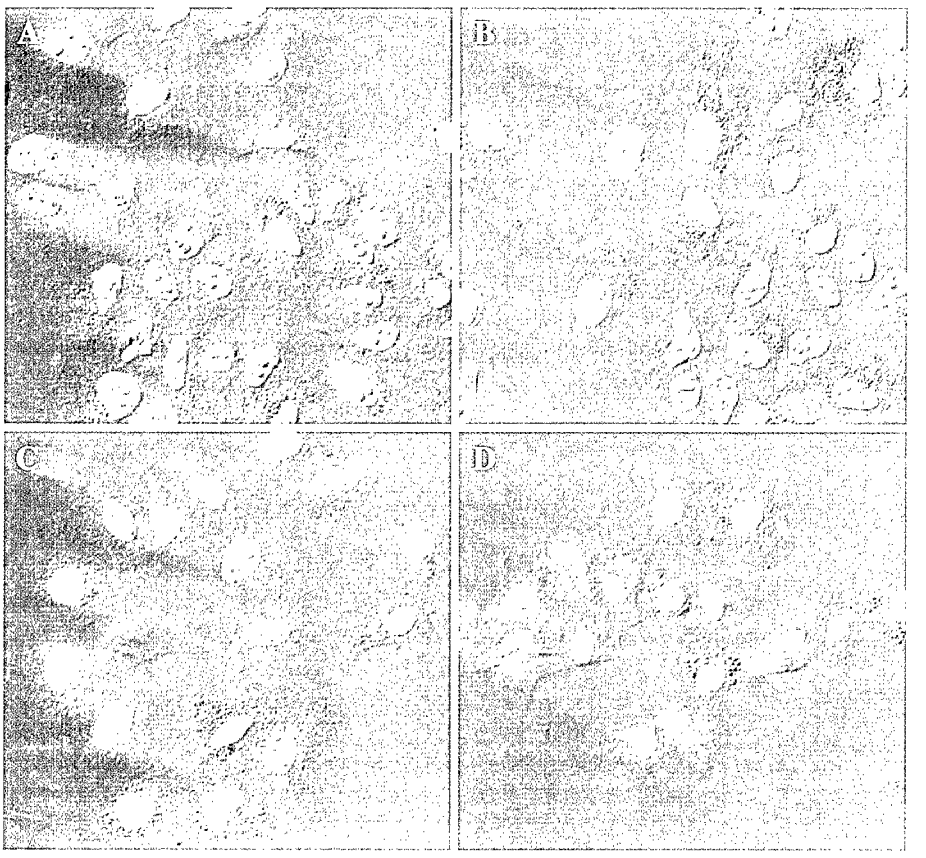

Fig. 2. Intracellular delivery of ODN to KB cells via the FR-targeted lipid vesicles. KB cells were treated with FR-targeted lipidic sODN for 5 min (Panel B), 15 min (Panel C) or 1 h (Panel D). Control cells were treated with ODN formulated in ligand-free lipid vesicles for 2 h (Panel A). Intracellular distribution of Cy3-labeled sODN was then examined under a confocal fluorescence microscope. The green color represents the SYTOX Green-stained nuclei, while the reddish color represents the Cy3-sODN.

After another 48 h cytotoxicity was examined by MTT assay.

2.11. Statistical analysis

Data were expressed as mean ± standard deviation (S.D.) and analyzed by the two-tailed unpaired Student's *t*-test using the PRISM software program (GraphPad Software, San Diego, CA). Data were considered significant if $P < 0.05$ (*).

3. Results

3.1. ODN formulated in FR-targeted lipid vesicles were efficiently protected from degradation by nucleases

FR-targeted, ODN-containing lipid vesicles were prepared as previously described [10]. One mol% of DSPE–PEG–folate was used as this consistently gave rise to lipid vesicles that were efficiently taken up by KB cells [10]. For nuclease protection assay, ODN of PO backbone were used. As shown in Fig. 1, free ODN were rapidly degraded by nuclease S1. No intact ODN could be detected on PAGE gel

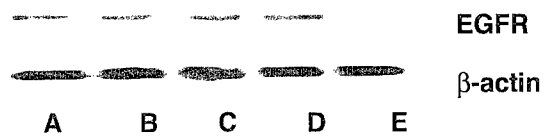

Fig. 4. Western analysis of EGFR expression in KB cells following targeted delivery of EGFR antisense ODN. Cells were treated with sODN (1), free or formulated in FR-targeted lipid vesicles for 1 h and then cultured in normal medium. Expression of EGFR in KB cells 4 days following ODN treatment was then examined by Western blotting using anti-EGFR antibody. A, KB cells without any treatment; B, KB cells treated with free control sODN; C, KB cells treated with control sODN formulated in FR-targeted lipid vesicles; D, KB cells treated with free EGFR antisense sODN (1); E, KB cells treated with antisense sODN (1) formulated in FR-targeted lipid vesicles.

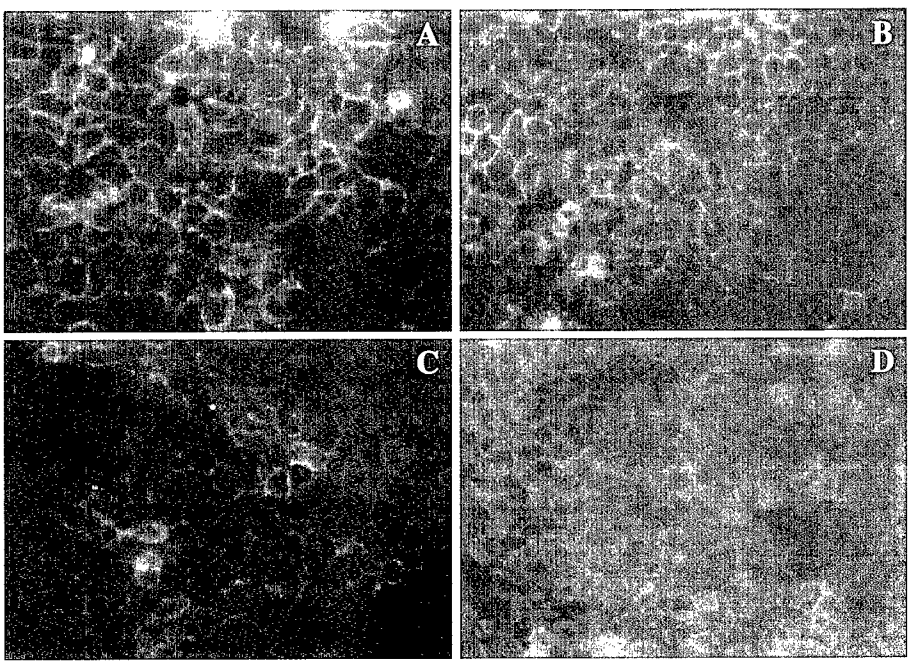

Fig. 3. Immunofluorescence analysis of EGFR expression in KB cells following targeted delivery of EGFR antisense ODN. Cells were treated with sODN, free or formulated in FR-targeted lipid vesicles for 1 h and then cultured in normal medium. Expression of EGFR in KB cells 4 days following ODN treatment was then examined by an indirect immunofluorescence staining using mouse anti-human EGFR antibody. A, KB cells without any treatment; B, KB cells treated with free EGFR antisense sODN (1); C, KB cells treated with control sODN formulated in FR-targeted lipid vesicles; D, KB cells treated with antisense sODN (1) formulated in FR-targeted lipid vesicles.

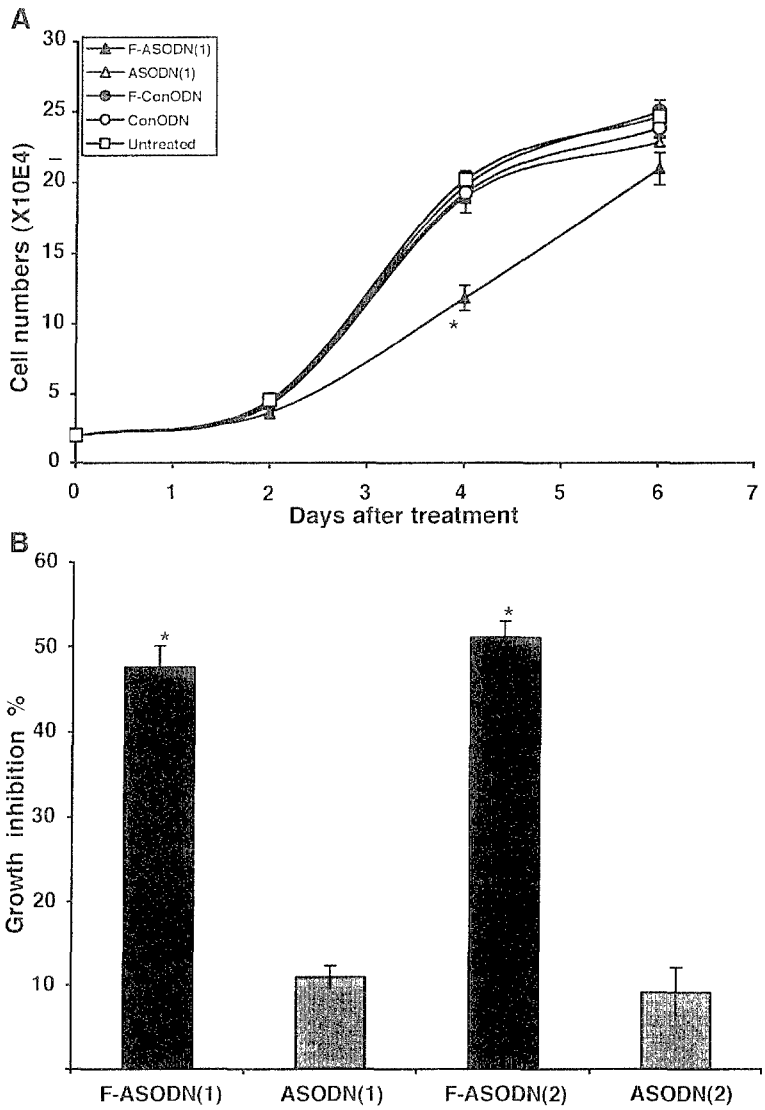

Fig. 5. Effect of single dosing of EGFR antisense ODN on the KB cell growth: KB cells were seeded to a 24-well plate at a cell density of 2×10^4 per well and allowed to grow overnight. sODN (1), free or formulated in FR-targeted lipid vesicles were added to the cells at a final concentration of 3 μM. Following incubation at 37 °C for 1 h, cells were washed with PBS twice and then continued to culture in normal medium and the cell numbers were counted at days 2, 4 and 6 (Panel A). In a separate experiment KB cells were seeded to a 96-well plate at a cell density of 0.5×10^3 per well and allowed to grow overnight. Cells then received sODN treatment as described above and the cytotoxicity was examined by a MTT colorimetric assay 4 days following ODN treatment (Panel B). ASODN (1), free EGFR antisense ODN (1); ASODN (2), free EGFR antisense ODN (2); F-ASODN (1), EGFR antisense sODN (1) formulated in FR-targeted lipid vesicles; F-ASODN (2), EGFR antisense sODN (2) formulated in FR-targeted lipid vesicles. ConODN, control sODN; F-ConODN, control sODN formulated in FR-targeted lipid vesicles. *$P < 0.05$ (vs. free ODN).

even 5 min following incubation with the nuclease. In contrast, ODN formulated in FR-targeted lipid vesicles were fully protected from the degradation by nuclease S1. Greater than 90% of the vesicle-associated ODN remained intact 30 min following incubation with nuclease S1 suggesting that ODN were largely encapsulated inside the lipid vesicles.

3.2. Efficient intracellular delivery of ODN to KB cells via the FR-targeted lipid vesicles

It has been previously shown that FR-targeted lipidic ODN were selectively taken up by KB cells that overexpress FR [10]. In this study, intracellular distribution of the sODN was further examined under a confocal fluorescence microscope at different times following addition of FR-targeted lipidic sODN to KB cells (Fig. 2). Binding of lipidic sODN to KB cells and their internalization were observed as early as 5 min following addition to the cells (Panel B). The cell-associated fluorescence intensity increased with time (Panels B–D). Interestingly, in addition to their increase in cytoplasmic distribution, sODN were also found to be accumulated in the nucleus in a time-dependent manner (Panels B–D). In contrast there was little cellular uptake by KB cells when sODN were formulated in ligand-free lipid vesicles (Panel A).

3.3. Down-regulation of EGFR expression in KB cells following targeted delivery of EGFR antisense ODN

Two antisense ODN [sODN (1) and sODN (2)] were examined in this study. Both sequences have been shown to be effective in down-regulating EGFR expression in tumor cells when given for a prolonged period of time [11,12]. In this study cells were treated with sODN (free or formulated in FR-targeted lipid vesicles) for only 1 h and then cultured in normal medium for 4 days. A short-term treatment was employed to mimic the in vivo situation where systemically administered ODN are expected to have limited interactions with tumors. Fig. 3 shows the expression of EGFR in KB cells following treatment with sODN (1), free or formulated in FR-targeted lipid vesicles. Incubation of KB cells with free sODN for a short period of time had minimal effect on EGFR expression (Panel B). Control sODN, formulated in FR-targeted lipid vesicles, had no effect either on EGFR expression (Panel C). In contrast, a dramatic reduction in EGFR expression occurred when KB cells were treated with the sODN (1) that were formulated in FR-targeted lipid vesicles (Panel D). Similar results were found for sODN (2) (data not shown). Down-regulation of EGFR following sODN treatment was further confirmed by Western analysis (Fig. 4). Again, FR-targeted antisense sODN but not

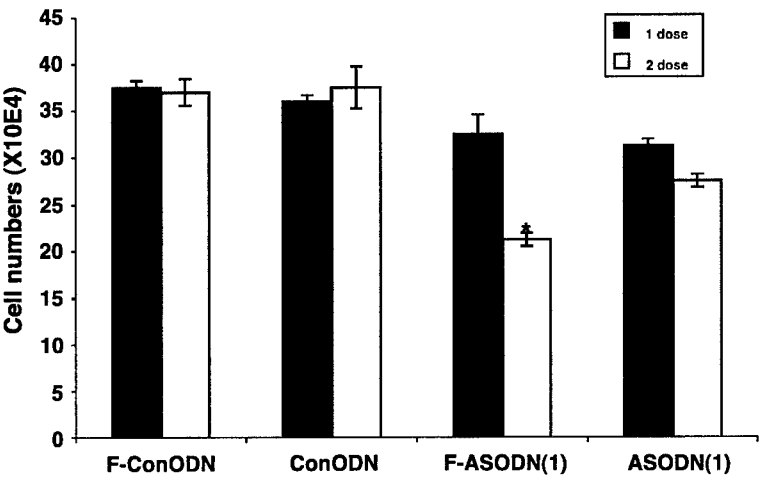

Fig. 6. Effect of repeated dosing of EGFR antisense ODN on the KB cell growth: KB cells were seeded to a 24-well plate at a cell density of 2×10^4 per well and allowed to grow overnight. Cells then received sODN treatment as described in the legend to Fig. 5 twice at days 0 and 3, and the cell numbers were counted at day 7. $^*P < 0.05$ (vs. single dose).

other controls significantly inhibited EGFR expression. In contrast, no significant difference was found among these groups with respect to β-actin levels (Fig. 4).

3.4. Effect of antisense treatment on the cell growth of KB cells

Fig. 5A shows the growth curve of KB cells at different times following a single treatment with EGFR antisense sODN (1), free or formulated in FR-targeted lipid vesicles. There was a significant growth inhibition at day 4 in the cells treated with FR-targeted antisense sODN compared to cells treated with control sODN, free or formulated in FR-targeted lipid vesicles. Free antisense sODN had no effect either in inhibiting the KB cell growth (Fig. 5A). MTT colorimetric assay (Fig. 5B) confirmed the results of trypan blue assay (Fig. 5A). Incorporation of either sODN (1) or sODN (2) into FR-targeted lipid vesicles resulted in a dramatic increase in their biological activity (Fig. 5B). However, there was a rebound in KB cell growth thereafter and there was no significant difference in the cell numbers at day 6 between free sODN group and the group treated with FR-targeted lipidic

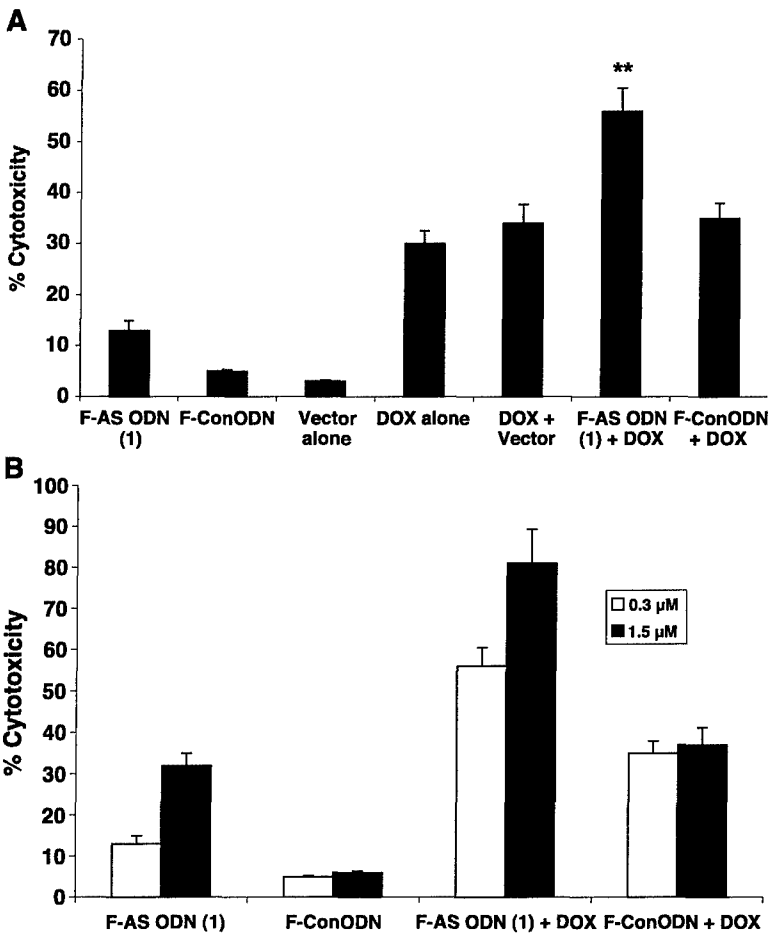

Fig. 7. Targeted delivery of EGFR antisense ODN sensitizes KB cells to DOX treatment: KB cells were seeded to a 96-well plate and exposed to FR-targeted lipidic sODN at an ODN concentration of 0.3 or 1.5 μM. Two days later cells were washed with PBS twice and then exposed to DOX in medium at a final concentration of 50 ng/ml. After another 48 h cytotoxicity was examined by MTT assay. Controls received treatment with FR-targeted lipidic ODN or DOX alone.

sODN (Fig. 5A). To examine whether a prolonged tumor growth inhibition can be achieved by repeated dosing, KB cells were treated with EGFR antisense or control sODN at days 0 and 3 and the cell numbers were counted at day 7. As shown in Fig. 6, repeated dosing was much more efficient than single dosing in inhibiting the KB cell growth. Control sODN, free or formulated in FR-targeted lipid vesicles, were not effective in inhibiting the tumor cell growth (Fig. 6). There was no significant difference either between antisense and control group in cell numbers at day 7 when cells received only a single treatment (Fig. 6).

3.5. Targeted delivery of EGFR antisense ODN sensitizes KB cells to DOX treatment

It has been shown that inhibition of EGFR function can sensitize cancer cells to chemotherapy [11,15]. In this study studies were conducted to whether targeted delivery of EGFR antisense ODN can similarly sensitize KB cells to DOX, a commonly used anticancer drug. Fig. 7 shows the effect on KB cells of treatment with EGFR antisense sODN, DOX, or a combination of both. FR-targeted antisense sODN, at a concentration of 0.3 μM, had minimal effect on the growth of KB cells. DOX, at the concentration of 50 ng/ml, only had a moderate inhibitory effect on KB cell growth. However, the combination of the two treatments resulted in a significant improvement in the inhibition of KB cell growth (Fig. 7A). The sensitizing effect of antisense treatment appears to be dose-dependent since increasing the dose of FR-targeted antisense sODN led to an increase in the inhibitory effect of the combination therapy (Fig. 7B). Control ODN formulated in lipid vector or lipid vector alone had no effect in sensitizing the DOX treatment (Fig. 7A).

4. Discussion

The present study confirmed the work of Semple and colleagues [9] that ODN can be quantitatively incorporated into lipid vesicles via a method that utilizes an ionizable aminolipid and an ethanol-containing buffer system. It has also extended their work by demonstrating that a targeting ligand can be incorporated into the lipid vesicles to improve the intracellular delivery of ODN to target cells. The lipidic ODN were fully protected from the degradation by nucleases (Fig. 1) suggesting that ODN were largely encapsulated inside the lipid vesicles.

Folate was chosen as a targeting ligand since FRs have been shown to be overexpressed in a number of cancer cells. Folate has been used successfully in targeting to tumors various types of agents including chemotherapeutic drugs [16], radionucleotides [17,18], ODN [5,19], DNA [20–22], etc. The advantages of the folate-targeting system include its excellent safety profile and the low immunogenicity. FRs have also been shown to mediate efficient internalization of free folate or the conjugates, which should facilitate intracellular delivery of the therapeutic agents.

Imaging studies showed that ODN formulated in FR-targeted lipid vesicles were efficiently taken up by KB cells (Fig. 2). Also noted is that ODN were accumulated in the nucleus in a time-dependent manner (Fig. 2) suggesting that ODN were efficiently released into cytosol from endosome following endocytosis. The mechanism by which ODN were escaped from endosomes is not clearly understood at present. This may be due to the pH-sensitive nature of DODAP since it has a pK_a around 6.5. A previous study by Budker et al. [23] has shown that cationic, pH-sensitive liposomes mediate transfection in an endosome acidification-dependent manner. It has been speculated that charged lipids may segregate from neutral lipids when mixing cationic liposomes with plasmid DNA [24]. Likewise, it was speculated that pH-sensitive cationic lipids may dissociate from the vector when they become fully charged, such as in the acidic endosomal environment [24]. Released cationic lipids may then participate in the process of endosome disruption via their detergent properties. ODN formulated in the DODAP-based lipid vesicles may be escaped from endosomes via a similar mechanism. The released ODN in the cytosol were then transported to the nucleus due to their efficient translocation across the nuclear membrane [25]. More studies are required to better understand the mechanism of endosomal escape.

After demonstrating efficient intracellular delivery of ODN via the FR-targeted lipid vesicles, their

therapeutic application was then investigated using anti-EGFR ODN as a model. EGFR is overexpressed in a variety of human cancers including KB cells [26] and EGFR signaling has been shown to cause increased proliferation, decreased apoptosis, and enhanced tumor cell motility and neoangiogenesis [27–29]. EGFR antisense ODN have been developed as a new therapeutics for the treatment of cancers that overexpress EGFR [11,12]. In this study, it was examined whether improving the intracellular delivery of EGFR antisense ODN via FR-targeted lipid vesicles will lead to an improved anti-tumor activity. A short-term treatment (1 h pre-incubation) was adapted to mimic the in vivo situation since systemically administered lipidic ODN are expected to have limited interaction with tumors. Fig. 5 shows that targeted delivery of anti-EGFR ODN to KB cells led to a significant growth inhibition, much more efficient than free ODN or ODN formulated in ligand-free lipid vesicles. The antitumor effect was transient and there was a rebound in cell growth after a maximal inhibition at day 4 (Fig. 5A). Similar observations were found in other studies [5]. However, sustained growth inhibition can be achieved via repeated dosing (Fig. 6). Eventually EGFR antisense therapy can be combined with other therapies such as chemotherapy to achieve better therapeutic effects [11]. As shown in Fig. 7, targeted delivery of EGFR antisense ODN greatly enhanced the sensitivity of KB cells to DOX treatment. A much lower dose of DOX was required to achieve an efficient tumor cell killing in the combination treatment group. Thus combination of chemotherapy with EGFR antisense treatment is expected to maximize the antitumor effect while minimizing the chemodrug-related toxicity.

Targeted delivery of anti-EGFR ODN to KB cells has previously been demonstrated with neutral liposomes conjugated with folate. The potential advantages of the new vector compared to the former formulation include (a) significantly improved ODN entrapment efficiency, and possibly (b) efficient release of ODN from endosome into cytosol. Interestingly, despite improved intracellular delivery of ODN to KB cells in vitro, the folate-conjugated neutral liposomes failed to improve the delivery of ODN to established KB tumor in intact mice [19]. It remains to be tested whether the new vector reported in this study can efficiently mediate delivery of ODN to target cells in vivo.

In summary, a novel lipid vector has been developed that is highly efficient in delivering ODN to tumor cells that overexpress FR. Delivery of anti-EGFR ODN via this vector resulted in down-regulation of EGFR expression in KB cells and growth inhibition. This formulation may hold promise for targeted delivery of antisense ODN for the treatment of tumors that overexpress FR.

Acknowledgements

This work was supported by DOD grant PC001525 and NIH grant HL RO1 63080 (to S. Li). The help from Dr. Simon Watkins in confocal study is greatly acknowledged.

References

[1] S. Agrawal, E.R. Kandimalla, Antisense and/or immunostimulatory oligonucleotide therapeutics, Curr. Cancer Drug Targets 1 (2001) 197–209.

[2] N. Dias, C.A. Stein, Potential roles of antisense oligonucleotides in cancer therapy. The example of Bcl-2 antisense oligonucleotides, Eur. J. Pharm. Biopharm. 54 (2002) 263–269.

[3] C.F. Bennett, M.Y. Chiang, H. Chan, J.E. Shoemaker, C.K. Mirabelli, Cationic lipids enhance cellular uptake and activity of phosphorothioate antisense oligonucleotides, Mol. Pharmacol. 41 (1992) 1023–1033.

[4] F. Cumin, F. Asselbergs, M. Lartigot, E. Felder, Modulation of human prorenin gene expression by antisense oligonucleotides in transfected CHO cells, Eur. J. Biochem. 212 (1993) 347–354.

[5] S. Wang, R.J. Lee, G. Cauchon, D.G. Gorenstein, P.S. Low, Delivery of antisense oligodeoxyribonucleotides against the human epidermal growth factor receptor into cultured KB cells with liposomes conjugated to folate via polyethylene glycol, Proc. Natl. Acad. Sci. USA 92 (1995) 3318–3322.

[6] D.C. Litzinger, J.M. Brown, I. Wala, S.A. Kaufman, G.Y. Van, C.L. Farrell, D. Collins, Fate of cationic liposomes and their complex with oligonucleotide in vivo, Biochim. Biophys. Acta 1281 (1996) 139–149.

[7] S. Li, L. Huang, Lipidic supramolecular assemblies for gene transfer, J. Liposome Res. 6 (1996) 589–608.

[8] K. Maruyama, In vivo targeting by liposomes, Biol. Pharm. Bull. 23 (2000) 791–799.

[9] S.C. Semple, S.K. Klimuk, T.O. Harasym, N. Dos Santos, S.M. Ansell, K.F. Wong, N. Maurer, H. Stark, P.R. Cullis, M.J. Hope, P. Scherrer, Efficient encapsulation of antisense

oligonucleotides in lipid vesicles using ionizable aminolipids: formation of novel small multilamellar vesicle structures, Biochim. Biophys. Acta 1510 (2001) 152–166.
[10] W. Zhou, X. Yuan, A. Wilson, L. Yang, M. Mokotoff, B. Pitt, S. Li, Efficient intracellular delivery of oligonucleotides formulated in folate receptor-targeted lipid vesicles, Bioconjug. Chem. 13 (2002) 1220–1225.
[11] F. Ciardiello, R. Caputo, T. Troiani, G. Borriello, E.R. Kandimalla, S. Agrawal, J. Mendelsohn, A.R. Bianco, G. Tortora, Antisense oligonucleotides targeting the epidermal growth factor receptor inhibit proliferation, induce apoptosis, and cooperate with cytotoxic drugs in human cancer cell lines, Int. J. Cancer 93 (2001) 172–178.
[12] J.R. Grandis, A. Chakraborty, Q. Zeng, M.F. Melhem, D.J. Tweardy, Downmodulation of TGF-alpha protein expression with antisense oligonucleotides inhibits proliferation of head and neck squamous carcinoma but not normal mucosal epithelial cells, J. Cell. Biochem. 69 (1998) 55–62.
[13] M. Ashida, T. Bito, A. Budiyanto, M. Ichihashi, M. Ueda, Involvement of EGF receptor activation in the induction of cyclooxygenase-2 in HaCaT keratinocytes after UVB, Exp. Dermatol. 12 (2003) 445–452.
[14] S. Li, A.R. Khokhar, R. Perez-Soler, L. Huang, Improved antitumor activity of *cis*-Bis-neodecanoato-*trans*-*R*, *R*-1,2-diaminocyclo-hexaneplatinum (II) entrapped in long-circulating liposomes, Oncol. Res. 7 (1995) 611–617.
[15] M.C. Prewett, A.T. Hooper, R. Bassi, L.M. Ellis, H.W. Waksal, D.J. Hicklin, Enhanced antitumor activity of anti-epidermal growth factor receptor monoclonal antibody IMC-C225 in combination with irinotecan (CPT-11) against human colorectal tumor xenografts, Clin. Cancer Res. 8 (2002) 994–1003.
[16] R.J. Lee, P.S. Low, Folate-mediated tumor cell targeting of liposome-entrapped doxorubicin in vitro, Biochim. Biophys. Acta 1233 (1995) 134–144.
[17] C.J. Mathias, S. Wang, R.J. Lee, D.J. Waters, P.S. Low, M.A. Green, Tumor-selective radiopharmaceutical targeting via receptor-mediated endocytosis of gallium-67-deferoxamine-folate, J. Nucl. Med. 37 (1996) 1003–1008.
[18] W. Guo, G.H. Hinkle, R.J. Lee, 99mTc-HYNIC-folate: a novel receptor-based targeted radiopharmaceutical for tumor imaging, J. Nucl. Med. 40 (1999) 1563–1569.
[19] C.P. Leamon, S.R. Cooper, G.E. Hardee, Folate-liposome-mediated antisense oligodeoxynucleotide targeting to cancer cells: evaluation in vitro and in vivo, Bioconjug. Chem. 14 (2003) 738–747.
[20] L. Xu, K.F. Pirollo, E.H. Chang, Tumor-targeted p53-gene therapy enhances the efficacy of conventional chemo/radiotherapy, J. Control. Release 74 (2001) 115–128.
[21] J.A. Reddy, C. Abburi, H. Hofland, S.J. Howard, I. Vlahov, P. Wils, C.P. Leamon, Folate-targeted, cationic liposome-mediated gene transfer into disseminated peritoneal tumors, Gene Ther. 9 (2002) 1542–1550.
[22] M.A. Gosselin, W. Guo, R.J. Lee, Incorporation of reversibly cross-linked polyplexes into LPDII vectors for gene delivery, Bioconjug. Chem. 13 (2002) 1044–1053.
[23] V. Budker, V. Gurevich, J.E. Hagstrom, F. Bortzov, J.A. Wolff, pH-sensitive, cationic liposomes: a new synthetic virus-like vector, Nat. Biotechnol. 14 (1996) 760–764.
[24] R.J. Lee, L. Huang, Lipidic vector systems for gene transfer, Crit. Rev. Ther. Drug Carrier Syst. 14 (1997) 173–206.
[25] O. Zelphati, F.C. Szoka Jr., Mechanism of oligonucleotide release from cationic liposomes, Proc. Natl. Acad. Sci. USA 93 (1996) 11493–11498.
[26] Y.H. Xu, N. Richert, S. Ito, G.T. Merlino, I. Pastan, Characterization of epidermal growth factor receptor gene expression in malignant and normal human cell lines, Proc. Natl. Acad. Sci. USA 81 (1984) 7308–7312.
[27] G. Carpenter, S. Cohen, Epidermal growth factor, J. Biol. Chem. 265 (1990) 7709–7712.
[28] T. Hunter, Cooperation between oncogenes, Cell 64 (1991) 249–270.
[29] C.L. Arteaga, Epidermal growth factor receptor dependence in human tumors: more than just expression? Oncologist 7 (2002) 31–39.

International Journal of Cancer (in press)

Anisamide-Targeted Stealth Liposomes: A Potent Carrier for Targeting Doxorubicin to Human Prostate Cancer Cells

Rajkumar Banerjee[#], Pradeep Tyagi, Song Li*, and Leaf Huang*
Center for Pharmacogenetics, School of Pharmacy, University of Pittsburgh, Pittsburgh, Pennsylvania 15213

Running Title: Anisamide-targeted stealth liposomes

*Address correspondence to:

Dr. Leaf Huang
Center for Pharmacogenetics
School of Pharmacy
633 Salk Hall
University of Pittsburgh
Pittsburgh, PA 15213, USA
(412) 648-9667 (voice)
(412) 648-1664 (fax)
huangl@msx.upmc.edu (Email)

or
Dr. Song Li
Center for Pharmacogenetics
University of Pittsburgh
School of Pharmacy
639 Salk Hall
Pittsburgh, PA 15213, USA
412-383-7976 (voice)
sol4@pitt.edu (Email)

[#]Present address: Division of Lipid Science and Technology, Indian Institute of Chemical Technology, Hyderabad 500 007, India

ABSTRACT

Certain human malignancies including prostate cancer overexpress sigma receptor, a membrane bound protein that binds haloperidol and various other neuroleptics with high affinity. An anisamide derivatized ligand possesses high affinity for sigma receptors and we hypothesized that its incorporation into the liposomes encapsulating Doxorubicin (DOX) can specifically target and deliver the drug to prostate cancer cells that overexpress sigma receptors. A polyethylene glycol phospholipid was derivatized with an anisamide ligand, which was then incorporated into the DOX-loaded liposome. The resulting anisamide-conjugated lipoosmal DOX showed significantly higher toxicity to DU-145 cells than non-targeted liposomal DOX, the IC50 being 1.8 μM and 14 μM respectively. The cytotoxicity of the targeted liposomal DOX, however, was significantly blocked by haloperidol, suggesting that the enhanced cytotoxicity was specifically mediated by the sigma receptors. Fluorescence imaging studies following intravenous administration showed that incorporation of anisamide into liposomes significantly improved their accumulation into the tumor. A weekly injection of the targeted liposomal DOX for four weeks at a dose of 7.5 mg/kg led to a significant growth inhibition of established DU-145 tumor in nude mice with minimal toxicity. Free DOX was effective, but associated with significant toxicities. The present study is the first to demonstrate the use of small molecular weight ligand for mediating efficient targeting of liposomal drugs to sigma receptor expressing prostate cancer cells both *in vitro* and *in vivo*.

Keywords: sigma receptor, prostate cancer, anisamide, PEG-liposome, drug-targeting.

INTRODUCTION

Sigma receptors are well known membrane-bound proteins, which show high affinity for neuroleptics (1). These receptors are expressed on normal tissues, such as liver, endocrine glands, kidneys, lungs, gonads, central nervous system and ovaries (2,3). Physiological role of these receptors in these normal tissues is largely unknown so far. Interestingly, a diverse set of human tumors, such as melanoma, non-small cell lung carcinoma, breast tumors of neural origin, and prostate cancer overexpress sigma receptors (4-10). Also interesting is the observation that benzamides exhibit a high affinity to sigma receptor expressing cells. This suggests the prospect of using these sigma-receptor binding ligands for the diagnosis and targeted therapy of a variety of tumors including prostate cancer (9,10). Indeed, several novel benzamide derivatives have been developed that show promise as tumor-imaging agents (9,10). However, sigma ligand has not yet been used to target anticancer drugs to tumors.

Liposomes have long been used as a vehicle for targeting drugs and other biologically active molecules. Monoclonal antibody can be conjugated to liposomes. The resulting immunoliposome showed specific targeting to tumor cells both *in vitro* (11-13) and in animal models (14-17). The triggered release property of the immunoliposome is further improved by designing pH-sensitive immunoliposome (18,19), heat-sensitive immunoliposome (20), and target-sensitive immunoliposome (21). We have also shown that the stealth property that arises by the inclusion of grafted polyethyleneglycol (PEG) can be added to the immunoliposome to further improve its *in vivo* targeting efficiency (22). Such liposome has been used to deliver anticancer drugs to the pulmonary metastatic tumor cells (23,24).

In this study, we have investigated whether small molecular weight anisamide can be used as a ligand to target liposomal drugs to sigma receptor overexpressing prostate cancer cells. These

anisamide molecules are chemically conjugated with phospholipids with a polyethylene glycol (PEG) spacer in-between. These ligand-conjugated PEG lipids are included along with other neutral lipids to form long circulating and targeted liposomes. It is expected that a properly designed ligand with high and selective affinity for the sigma receptor will allow efficient interaction with sigma receptor expressing cells subsequent to incorporation of the ligand on the liposome surface. This formulation has an added advantage of stabilizing the encapsulated drug because PEG is known to prolong the circulation times of the liposome *in vivo* (25,26). To this end, we have incorporated an anisamide derivatized PEG-phospholipid in the liposome formulation with the anisamide ligand protruding on the liposome surface via a PEG spacer. We have studied the binding of this liposome to the human prostate carcinoma cells, and the drug delivery properties of this novel targeted liposome in a xenograft animal tumor model.

MATERIALS AND METHODS

Chemicals and General Procedures:

Phospholipids such as palmitoleylphosphatidyl choline (POPC), DSPE-PEG(2000)-OCH_3 and rhodamine-PE were purchased from Avanti Polar Lipids (Birmingham, Al). DSPE-PEG(3400)-NH_2 (purity, >70% by wt) was a generous gift from NOF Corporation, Japan and was used without further purification. Cholesterol, Sepharose-4B, trypsin-EDTA solution, 3-(4,5-dimethylthiazol-2-yl)-2,5-diphenyltetrazolium bromide (MTT), dimethylsulfoxide (DMSO) were purchased from Sigma Chemical Co. (St. Louis, MO). All the chemicals and organic solvents required for synthesis were purchased from either Aldrich (Milwaukee, WI) or Fisher Scientific (Pittsburgh, PA). They were used without further purification. DOX was purchased from either Aldrich or ICN Biomedicals (Aurora, OH). ^1H NMR spectra were recorded on a Bruker FT 300 MHz and Varian FT 400 MHz instrument.

Cell Culture:

DU-145 human prostate adenocarcinoma cell line was purchased from American Type Culture Collection (Rockville, MD) and was mycoplasma free. Cells were cultured in MEM medium (ATCC) containing 10% fetal bovine serum (Invitrogen, Carlsbad, CA) and 1% penicillin-streptomycin at 37^0C in a humidified atmosphere of 5% CO_2 in air. Cultures of 85-90% confluency were used for all of the experiments. The cells were trypsinized, counted, subcultured into 96-well plates for viability studies, 6-well plates for liposome binding studies, and 4-well slide-plates for qualitative fluorescence microscopic studies. The cells were allowed to adhere overnight before using for experiments.

Syntheses of Ligands:

Synthesis of DSPE-PEG-SP3-AA: The synthesis was carried out according to the following synthetic scheme: A) The compound 4-methoxy-N-(2-oxo-ethyl)-benzamide (**I**) was obtained by two steps: i) reacting anisic acid (1.17 g, 8.2 mmole) with 2-aminoacetaldehydediethylacetal (1.0 g, 7.5mmole) in dicholoromethane and in the presence of DCC (1.7 g, 8.2 mmole), DMAP (500 mg, 4.09 mmol) for 24 h, followed by silica gel column chromatographic purification using ethyl acetate/Petroleum ether as eluting solvent mixture, ii) refluxing the resulting purified compound in 25 % aqueous solution in acetone at pH 2 for 1.5h, further neutralizing and extracting the aldehyde **I** with chloroform in organic phase. The overall yield was 77%. B) **I** (355 mg, 1.93 mmol) was refluxed under N_2 for 2 h with 4-aminobutyric acid (166.5 mg, 1.61 mmol) in dry methanol in the presence of anhydrous $MgSO_4$. The reaction mixture was cooled and to it sodium cyanoborohydride was added in excess and stirred as such for 2h. The compound 7-[2-(4-methoxy-benzylamino)-ethylamino]-heptanoic acid (**II**) was purified by silica gel column chromatography using methanol/chloroform eluting solvent mixture. The purified yield was 20%. All the intermediate products except **I** were characterized by NMR spectroscopy. C) Compound **II** (40 mg, 0.148 mmol) was reacted with DSPE-PEG-NH_2 (50 mg, 0.0125 mmol) in dichloromethane and in the presence of DCC (5 mg, 0.024 mmol) & DMAP (3 mg, 0.024 mmol) under N_2 at room temperature for 24 h. The dichloromethane was evaporated and the whole content was taken in acetone and kept at -20^0C. The product precipitated out. The yield of the PEG lipid was calculated based on the amount of phosphate determined in the mixture (yield = 50%). The overall reaction yield of DSPE-PEG-SP3-AA was 7%. During the liposome preparation (see below), the ligand-conjugated PEG-lipid was added according to the phosphate concentration. After the liposome formation the absorbance at 255nm (λ_{max} for anisamide,

ε=14832) was measured and from this value the absorbance value at 255nm for the ligand-free liposome was subtracted. The amount of ligand attached to the liposome was then calculated based on the difference in the absorbance at 255 nm.

Synthesis of DSPE-PEG-SP2-AA. The synthesis was carried out according to the following synthetic scheme. Briefly, N-(2-bromo-ethyl)-4-methoxy-benzamide [synthesized according to the published synthetic protocol (27)] (100 mg, 0.4 mmol) was reacted with DSPE-PEG-NH_2 (100 mg, 23.2 μmol) in acetonitrile (5 ml) in presence of DIPEA (30 μl, 0.2 mmol) at 65-70^{0}C for 8h. TLC shows the formation of new UV active product. Methanol was added to the mixture (5 ml) followed by excess ether (50 ml) and it was then kept at –80^{0}C for 24 h. The precipitate was collected following centrifugation and recrystallization was repeated twice. The overall yield was 70%. The product (single spot, Rf 0.7, 26:4 $CHCl_3$: Methanol), while eluting out at 2 ml/min through semi-preparative RP C_{18} Vydac column gave a peak R_T 6.4 (90% pure) in a isocratic gradient of acetonitrile (containing 0.1% TFA) to methanol in a ratio of 45:55. The product DSPE-PEG-SP2-AA was characterized by NMR and used without further purification. The integration of the protons in the aromatic moiety attached to high molecular weight PEG does not give accurate peak heights as opposed to other protons in NMR, as reported elsewhere (28).

Liposome Preparation:

Preparation of DOX-loaded liposomes: For DOX entrapment lipid films were prepared by drying the chloroform solution of a total of 11.61 μmol of POPC, cholesterol, and DSPE-PEG-SP2-AA or DSPE-PEG-SP3-AA or DSPE-PEG(2000)-OCH_3 under a gentle stream of N_2 and dried in vacuum for at least 6h. The lipid mixtures were composed of POPC:Chol:DSPE-PEG-

SP2-AA or POPC:Chol:DSPE-PEG-SP3-AA or POPC:Chol:DSPE-PEG(2000)-OCH_3 in a molar ratio of 61.6 : 36.5 : 2. It was hydrated with 1ml of 0.1M citrate pH 4.0 for DOX entrapment following the protocol as described (29). The DOX-entrapped liposome was finally gel-filtered through Sepharose-4B gel column using Hepes buffer to remove unencapsulated DOX (if any). The amount of DOX was quantitated by UV measurement at absorbance maximum of 495 nm (ε= 12500) for each of the liposomes entrapping DOX. The final DOX-liposome solutions contain 150 mM NaCl.

Preparation of rhodamine-PE containing liposomes: The lipid films were prepared by drying the chloroform solution of a total of 11.61 μmol of POPC, cholesterol, rhodamine-PE and DSPE-PEG-SP2-AA or DSPE-PEG-SP3-AA or DSPE-PEG(2000)-OCH_3 under a gentle stream of N_2 and further dried in vacuum for at least 6h. The lipid mixtures were composed of POPC:Chol:rhodamine-PE:DSPE-PEG-SP2-AA or POPC:Chol:rhodamine-PE:DSPE-PEG-SP3-AA or POPC:Chol:rhodamine-PE:DSPE-PEG(2000)-OCH_3 in a molar ratio of 61.1 : 36 : 1 : 2. It was incubated with 1ml Hepes buffered saline (HBS) and allowed to hydrate with occasional vortex and intermittent bath sonication for about 0.5h. The hydrated lipid suspension was extruded through 0.1μm pore size membrane in a manual extruder (Avestin Inc., Canada) for 10 times at 65^0C. The fluorescent liposomes were gel filtered through Sepharose-4B gel column eluted with HBS to remove the un-incorporated rhodamine-lipid or other impurities (if any). The liposome solution was collected in the void volume. The liposome solution was further filtered through 100,000 molecular weight cut-off membrane filter (Milipore Inc.) for 3h by centrifugation at 3000 rpm. The retained liposomal concentrate was collected and used for quantitative liposome uptake and fluorescence microscopic studies.

Immunofluorescence Microscopic Examination:

DU-145 cells were seeded at a density of 1 x 10^5 cells/ well in a 4-well Nalge Nunc Lab-Tek chamber slide (Naperville, IL) and kept for overnight at 37^0C. The cells were washed three times with PBS and incubated with various concentrations of rhodamine-labeled liposomes at 37^0C for 0.5h. Cells were washed with PBS three times and fixed in 3.7% paraformaldehyde in PBS for 15 min. The cells were washed again with PBS three times and the fluorescence images were taken at 200X magnification with a red filter in a Nikon fluorescence phase contrast optical microscope.

Liposome Uptake Study:

DU-145 cells (2.25 x10^5) were placed in 6-well cell culture plates and allowed to attach and grow overnight at 37^0C and 5% CO_2 in air. Cells were washed with PBS three times and incubated with various concentrations of rhodamine-labeled liposomes for 4h at 37^0C. The treatments were done in triplicates. The cells were then washed with PBS three times and lysed with 1 ml of 0.1% Triton-X-100 in PBS. The lysates were collected and measured for the fluorescence intensity at λ_{em} = 581 nm and λ_{ex} = 560 nm in a Perkin Elmer LS50B Luminescence Spectrometer (Norwalk, CT). The results are expressed as arbitrary fluorescence intensity/mg of protein lysates. For inhibition study, cells were preincubated for 2h with 2 ml of 30 μM of HP in complete media and liposome uptake study was similarly performed as described above.

Cytotoxicity:

The cytotoxic effect of free DOX and DOX encapsulated in targeted liposome or non-targeted liposome was assayed by a MTT colorometric assay. DU-145 cells were seeded at a density of 5,000 cells/well (200 μl) in 96-well flat-bottomed microtiter plates overnight. Cells were washed with PBS once and incubated with various concentrations of free DOX or different liposomal DOX in triplicate for 2h at 37^0C. The cells were washed three times with PBS at the end of incubation and further incubated for 48h in a drug-free condition. 20 μl of MTT solution (5 mg/ml in PBS) was then added to each well and the cells were incubated further for 1h at 37^0C. The media were removed and the cells were dissolved in DMSO. UV absorbance at 555 nm was measured in Ultramark Microplate Imaging System (BIO-RAD). The data are expressed as the percent of viable cells compared to untreated control cells. For the HP inhibition study, cells were preincubated in 30μM HP (200 μl) in complete media for 2h before the addition of drugs and the cytotoxicity was similarly evaluated as described above.

Animals and Tumor Model:

Three to four weeks old female athymic nu/nu (Harlan Sprague Dawley, Indianapolis, Indiana) were used for all animal experiments. Subcutaneous (SC) tumors were established by injecting 1.5 x 10^6 DU-145 cells in the right flank of the abdomen region. Care and maintenance of animals were done in University of Pittsburgh Central Animal Facility and in adherence to Institutional guidelines of the Institutional Animal Care and Use Committee (IACUC).

Microscopic Imaging of Tumor Sections:

Nude mice bearing DU-145 tumor in the size of 70-80 mm^2 were used in this study. They received the following treatments: 1) HBS; 2) rhodamine labeled liposome containing 2 mole% DSPE-PEG-SP2-AA (total lipid 2.32 μmol); 3) rhodamine labeled liposome containing 2 mole% DSPE-PEG-OCH_3 (total lipid 2.32 μmol). At 2, 4, and 24 h following injection, mice were sacrificed and tumors were collected, frozen in TBS tissue-freeze medium (Triangle Biomedical Sciences, Durham, N.C.) and sectioned into 5 μm thin sections using a HM 505 E MICROM Cryostat. Similarly, for the study of DOX uptake by the tumor, mice received the following treatments: 1) HBS; 2) DOX-liposome (7.5 mg DOX/kg) containing DSPE-PEG-OCH_3; and 3) DOX-liposome (7.5 mg DOX/kg) containing DSPE-PEG-SP2-AA. After 24 h the mice were sacrificed and tumors removed were sectioned after freezing. Fluorescence images from all of the tissue sections were directly taken at 200X magnification with red filters in a Nikon fluorescence phase contrast optical microscope to examine the rhodamine liposome and DOX uptake in the tumor.

Therapeutic Studies:

Groups of five nude mice bearing SC tumor were included in this study. They received the following treatments: a) HBS (untreated group), b) DOX-liposome containing DSPE-PEG-SP2-AA (DSPE-PEG-SP2-AA group), c) DOX-liposome containing DSPE-PEG-OCH_3 (DSPE-PEG-OCH_3 group), and d) free DOX (free DOX group). Mice received weekly i.v. injection and the DOX dose was 7.5 mg/kg. The tumor size was measured twice a week.

Statistical Analysis:

Data were expressed as mean ± standard derivation and statistical analysis was done by two-tailed unpaired Student t-test using the PRISM software program (GraphPad Software, San Diego, CA). Data were considered significant if $p < 0.05$.

RESULTS

Syntheses of phospholipid-PEG-anisamide conjugates:

Anisamide was chosen in this study as a targeting ligand (5). In order to attach the anisamide moiety to liposomes, we have synthesized a phospholipid conjugate. A PEG (M.W. 3,500) spacer was included between lipid and anisamide to improve the targetability. Figure 1 shows the scheme for the synthesis of anisamide-derivatized phospholipids. The inclusion of a secondary amine in the position two carbons away from the amide-nitrogen of the benzamide analogue (here, anisamide) has been shown to increase the receptor affinity of the ligand (30). The relatively poor overall yield of DSPE-PEG-SP3-AA (7%) prompted us to design DSPE-PEG-SP2-AA. The active ligand moiety remained the same for both molecules. The overall reaction yield of the DSPE-PEG-SP2-AA formation was ten fold greater than that of the DSPE-PEG-SP3-AA.

Liposome uptake study:

Figure 2A shows the liposome uptake at 4 h following incubation with various concentrations of rhodamine-labeled liposome, non-targeted or conjugated with SP2-AA or SP3-AA. SP2-AA-targeted liposomes were most efficiently taken up by DU-145 cells. The non-targeted liposomes showed the least uptake. Liposomes containing DSPE-PEG-SP3-AA showed an intermediate level of uptake. The cellular uptake of targeted liposome was significantly inhibited by either pretreatment or co-treatment with HP, a known sigma antagonist (Figure 2B), suggesting that the enhanced cellular uptake of SP2-AA- or SP3-AA-targted liposomes was specifically mediated by the sigma receptors.

Figure 3 shows the fluorescence microscopic examination of the uptake of rhodamine-labeled liposomes by DU-145 cells. In agreement with data in Figure 2, cells treated with SP2-AA-targeted liposomes had the greatest amount of cell-associated fluorescence intensity, followed by cells treated with SP3-AA-targeted liposomes. Cells treated with non-targeted liposome had the least amount of cell-associated fluorescence intensity. At high magnification, SP2-AA-targeted liposomes were found to be associated with cell membrane as well as inside the cells (see supplemental Figure 1).

Targeted delivery of liposomal DOX via sigma receptor to prostate cancer cells:

The cytotoxicity of targeted or non-targeted liposomal DOX was examined on DU-145 cells. Liposome containing DSPE-PEG-SP2-AA was chosen in the cytotoxicity study as it was more efficiently taken up by DU-145 cells than the liposome containing DSPE-PEG-SP3-AA (Figures 2 & 3). Figure 4A shows that targeted liposomal DOX killed DU-145 cells more effectively than the non-targeted DOX at concentrations below 46 μM, with the IC_{50} of 1.8 μM and 14 μM in two groups, respectively. To further demonstrate the involvement of the sigma receptor in cell killing, DU145 cells were preincubated with 30 μM HP for 2h before the addition of liposomal DOX in the presence of haloperidol HP. Figure 4B illustrates that HP significantly inhibited the cytotoxicity of DOX encapsulated in the targeted liposome, but produced minimal effect in the cytotoxicity of non-targeted liposomal DOX, which led us to suggest that the enhanced killing effect in targeted liposomal DOX is mediated by sigma receptors. It is also evident from Figure 4A that free DOX was more potent in cell killing than liposomal DOX (targeted or non-targeted) and its cytotoxicity was not affected by HP.

Targeted delivery of rhodamine-labeled liposome to tumor in tumor bearing athymic nude mice:

As evident from cell culture experiments, DSPE-PEG-SP2-AA containing liposome was more efficient than SP3-AA-containing liposome in targeting and was thus used in all of the subsequent animal experiments. Figure 5 shows the distribution of the targeted or non-targeted rhodamine liposomes in tumors at 2, 4 and 24 h following i.v. injection. It is apparent that at all of the three time points of our study, the SP2-AA-targeted liposome accumulated in the tumor more efficiently compared to non-targeted liposome. Accumulation was highest at an early time point, i.e., 2 h, and gradually decreased with time.

Targeted delivery of liposomal DOX to tumor in athymic nude mice:

Red fluorescence emitted by DOX can be directly imaged in the tumor sections for measuring DOX accumulation in the tumor at different time points following i.v administration. Images in Figure 6 show that greater amounts of DOX accumulated in the tumor treated with DOX loaded in SP2-AA-targeted liposome compared to that treated with non-targeted liposome. Distribution of DOX loaded liposome is consistent with distribution of rhodamine-labeled liposome

Therapy of tumor by anisamide-conjugated liposomal DOX:

Figure 7 shows the result of tumor therapy. The treatment started on day 5 from post-inoculation of tumor cells. The injected dose of DOX for mice was fixed at 7.5 mg/kg in all of the treatment groups. The control group received HBS. The most potent antitumor activity without any association of obvious toxicity was seen in the mice treated with SP2-AA-targeted liposomal DOX. The free DOX also showed efficient tumor growth retardation, but caused significant toxicity to the mice: 2 out of 5 mice developed ascites on day 15; and 3 out of 5 died

on day 18 and the remaining died on day 22. There were no obvious toxicities in the other treatment groups with respect to body weight loss or development of ascites. The SP2-AA-targeted liposomal DOX showed most facile and statistically significant ($p<0.05$) tumor growth retardation compared to non-targeted liposomal DOX.

DISCUSSION

The sigma receptors are overexpressed in a variety of human tumors including prostate cancer cells (4-10), which makes sigma ligand a potentially interesting ligand to target drugs to such tumors. Also interesting is the observation that radioiodinated benzamides exhibit a high affinity to sigma receptor-positive cells (8, 10). These radiolabeled benzamides have been successfully used in imaging several types of cancers including prostate tumor in the mouse model (9). These studies suggest the possibility of using sigma-receptor binding ligands for the diagnosis of a variety of human tumors including prostate cancer (9,10). We have synthesized a benzamide analogue and demonstrated for the first time its therapeutic application towards targeting and killing prostate cancer cells. The benzamide derivatives are of small molecular weight and easy to modify according to the need of the delivery system. It can be directly attached to a phospholipid and incorporated in the liposome formulation. A PEG spacer can be included between lipid and benzamide to improve the ligand targetability. Inclusion of the PEG moiety also provides improved stability and increased circulation half-life of the liposome *in vivo* (25, 26).

In vitro studies demonstrated that anisamide (an analogue of benzamide) efficiently mediated targeting of liposome to DU-145 cells that overexpress sigma receptor. The cellular uptake was dependent on dose and required the necessary presence of the anisamide moiety in the phospholipid conjugate (Figures 2 &3). Data obtained from the uptake studies was corroborated by the DOX-mediated cytotoxicity studies. SP2-AA-targeted liposomal DOX showed increased cellular cytotoxicity over the non-targeted liposomal DOX (Figure 4A). The improved cellular uptake and cytotoxicity appeared to be mediated by sigma receptor as both were significantly inhibited by the presence of HP (Figures 2B and 4B)

The two anisamide-PEG derivatized phospholipids that are used in the current study differ by the spacer-length between the PEG and active moiety but both have a secondary amine two carbons away from the amide carbon. This amine has been shown to be critical for targeting of radioisotopes to sigma receptor-positive tumor cells (30). Our preliminary studies showed that this amine is also important for efficient targeting of liposomes: direct coupling of anisic acid to DSPE-PEG-NH_2 led to a conjugate that showed poor targeting to DU-145 cells (data not shown). It is interesting to note that DSPE-PEG-SP2-AA was more active than DSPE-PEG-SP3-AA in mediating liposome uptake (Figures 2A & B). The reason of this discrepancy is not clear at present. Further structure-activity studies may lead to more efficient sigma receptor targeting ligands.

It should be noted that despite the improved targeting, DOX formulated in liposomes containing DSPE-PEG-SP2-AA was less potent than free drug (Figure 4A). This might be due to the fact that the tumor cells were exposed to the drug for an extended period of time. Such condition, however, is unlikely to occur *in vivo* where the free drug is rapidly cleared following the administration. Similar observation has been found in the study reported by Iden and Allen (31) using antibody-targeted liposomal DOX.

The sigma receptor-mediated *in vivo* targeting was clearly demonstrated in the study with rhodamine labeled liposome. A more efficient accumulation of rhodamine liposome in the tumor (Figure 5) was seen in mice following i.v administration of SP2-AA-targeted liposome at all three time points examined (2, 4, and 24 h post injection). Similarly much more DOX was found to accumulate in the tumor for targeted liposomal DOX (Figure 6). Both targeted and non-targeted PEG liposomes are expected to extravasate into the tumor because of their extended half-life. The equilibrium of liposome movement in and out of the tumor is expected to shift

towards tumor uptake if the liposome is armed with an efficient targeting ligand. The inclusion of a targeting ligand could also improve the bioavailability of liposomal DOX by facilitating the subsequent internalization into tumor cells. These led to an overall improved accumulation of targeted liposomes in the tumor.

In vivo therapy studies clearly showed that the anisamide-targeted liposomal DOX efficiently inhibited the growth of established DU-145 tumors in mice. A number of studies have shown that entrapment of chemotherapeutic drugs into long-circulating liposomes significantly improves their therapeutic index. However, there have been conflicting results regarding whether active targeting can further improve the therapeutic efficacy of liposomal drugs (32, 33). Data from Figure 7 clearly indicate that anisamide-targeted liposomal DOX is more efficient than non-targeted liposomal DOX in inhibiting the growth of DU-145 prostate cancer cells. A much more significant difference was observed between the two groups when a lower dose of DOX was used (data not shown). Free DOX, although effective, was associated with significant levels of toxicity. Thus, anisamide-targeted liposomal DOX can efficiently inhibit the growth of established prostate cancer with minimal side effects.

Several targeted systems have been developed for targeted delivery of liposomal drugs to tumors. Most of them utilize antibodies as a ligand (31, 34). A few studies reported using small molecule ligands such as folate for targeted liposomal drug delivery (35, 36). Our studies suggest that benzamide and its derivatives show promise as a new type of small molecule ligand for targeting of various types of anticancer agents to sigma receptor-positive cancers. There are two potential advantages with our new system compared to existing targeting systems including: 1) low immunogenicity of benzamide and its other excellent safety profile, and 2) versatility due to the fact that various types of tumors overexpress sigma receptors. Thus, anisamide-targeted

drugs may become a novel class of therapeutics for the treatment of human cancers, which warrants further investigation.

ACKNOWLEDGEMENT

RB is generously supported by a post-doctoral research fellowship from SASS Foundation for Medical Research Inc. This study was partially supported by NIH grant CA74918 to L.H. and DOD grant PC001525 to S. L.

ABBREVIATIONS

POPC: 1,2-Dipalmitoleoyl-sn-Glycero-3-phosphatidylcholine

Chol: Cholesterol

DSPE-PEG(2000)-OCH_3: Distearoyl-sn-glycero-phosphatidylethanolamine-[ω-methoxy-polyethylene glycol(2000)]

DSPE-PEG-SP2-AA: Distearoylglycerolphosphatidylethanolamine-polyethylene glycol(3400)-ω–[2–(4'–methoxybenzamido)]ethylamine.

DSPE-PEG-SP3-AA: Distearoylglycerolphosphatidylethanolamine-polyethylene glycol(3400)-ω–[4–{ 2'–(4''–methoxybenzamido)]ethylamino}butamide.

DCC: Dicyclohexylcarbodiimide

DMAP: N, N-dimethylaminopyridine

HP: Haloperidol

PEG: Polyethylene glycol

MTT: 3-(4,5-dimethylthiazol-2-yl)-2,5-diphenyltetrazolium bromide

DMSO: Dimethyl sulfoxide

PBS: Phosphate buffered saline

DOX: DOX

HBS: Hepes buffered saline

References:

1. Walker JM, Bowen WD, Walker FO, Matsumoto RR, De Costa B, Rice KC. Sigma receptors: biology and function. Pharmacol. Rev.1990;42:355-402.
2. Wolfe SA. Jr, Culp SG, De Souza EB. Sigma-receptors in endocrine organs: identification, characterization, and autoradiographic localization in rat pituitary, adrenal, testis, and ovary. Endocrinology.1989;124:1160-72.
3. Hellewell SB, Bruce A, Feinstein G, Orringer J, Williams W, Bowen WD. Rat liver and kidney contain high densities of sigma 1 and sigma 2 receptors: characterization by ligand binding and photoaffinity labeling. Eur. J. Pharmacol.1994;268:9-18.
4. Vilner BJ, John CS, Bowen WD. Sigma-1 and sigma-2 receptors are expressed in a wide variety of human and rodent tumor cell lines. Cancer Res.1995;55:408-413
5. John CS, Bowen WD, Saga T, Kinuya, S, Vilner BJ, Baumgold J, Paik CH. Reba RC, Neumann RD, Varma VM. A malignant melanoma imaging agent: synthesis, characterization, *in vitro* binding and biodistribution of iodine-125-(2-piperidinylaminoethyl)4-iodobenzamide. J. Nucl. Med. 1993;34:2169-75.
6. John CS, Vilner BJ Bowen WD. Synthesis and characterization of [125I]-N-(N-benzylpiperidin-4-yl)-4- iodobenzamide, a new sigma receptor radiopharmaceutical: high-affinity binding to MCF-7 breast tumor cells. J. Med. Chem.1994;37:1737-9
7. John CS, Vilner BJ, Gulden ME, Efange SM, Langason RB, Moody TW, Bowen WD. Synthesis and pharmacological characterization of 4-[125I]-N-(N-benzylpiperidin-4-yl)-4-iodobenzamide: a high affinity sigma receptor ligand for potential imaging of breast cancer. Cancer Res.1995;55:3022-7.

8. John CS, Gulden ME, Vilner BJ, Bowen WD. Synthesis, *in vitro* validation and *in vivo* pharmacokinetics of [125I]N-[2-(4-iodophenyl)ethyl]-N-methyl-2-(1-piperidinyl) ethylamine: a high-affinity ligand for imaging sigma receptor positive tumors. Nucl. Med. Biol.1996; 23:761-6

9. John CS, Vilner BJ, Geyer BC, Moody T, Bowen WD. Targeting sigma receptor-binding benzamides as *in vivo* diagnostic and therapeutic agents for human prostate tumors. Cancer Res.1999; 59: 4578-83

10. John CS, Bowen WD, Fisher SJ, Lim BB, Geyer BC, Vilner BJ, Wahl RL. Synthesis, *in vitro* pharmacologic characterization, and preclinical evaluation of N-[2-(1'-piperidinyl)ethyl]-3-[125I]iodo-4-methoxybenzamide (P[125I]MBA) for imaging breast cancer. Nucl. Med. Biol.1999; 26:377-82.

11. Huang A, Huang L, Kennel SJ. Monoclonal antibody covalently coupled with fatty acid: a reagent for *in vitro* liposome targeting. J. Biol. Chem.1980;255: 8015-8018.

12. Huang A, Tsao YS, Kennel SJ, Huang L. Characterization of antibody covalently coupled to liposomes. Biochim. Biophys. Acta.1982;716:140-150.

13. Huang A, Kennel SJ, Huang L. Interactions of immunoliposomes with target cells. J. Biol. Chem.1983;258:4034-4040.

14. Hughes BJ, Kennel S, Lee R, Huang L. Monoclonal antibody targeting of liposomes to mouse lung *in vivo*. Cancer Res.1989;49:6214-6220.

15. Maruyama K, Takahashi N, Tagawa T, Nagaike K, Iwatsuru M. Immunoliposomes bearing polyethyleneglycol-coupled Fab' fragment show prolonged circulation time and high extravasation into targeted solid tumors in vivo. FEBS Lett.1997; 413:177-180.

16. Park JW, Hong K, Carter P, Asgari H, Guo LY, Keller GA, Wirth C, Shalaby R, Kotts C, Wood WI, Papahadjopoulos D, Benz CC. Development of Anti-p185^{HER2} Immunoliposomes for Cancer Therapy. Proc. Natl. Acad. Sci. *USA*.1995; 92:1327-1331

17. de Menezes DEL, Pilarski LM, AllenTM. in vitro and in vivo targeting of immunoliposomal DOX to human B-cell lymphoma. Cancer Res. 1998;58 : 3320-3330.

18. Connor J, Huang L. Efficient cytoplasmic delivery of a fluorescent dye by pH-sensitive immunoliposomes. J. Cell. Biol.1985;101:582- 589.

19. Connor J, Huang, L. pH- sensitive immunoliposomes as an efficient and target-specific carrier for antitumor drugs. Cancer Res.1986;46:3431-3435.

20. Sullivan SM, Huang L. Heat- sensitive immunoliposomes: preparation and characterization. Biochim. Biophys. Acta. 1985;*812*:116-126.

21. Ho RJY, Rouse B, Huang L. Target- sensitive immunoliposomes: preparation and characterization. Biochemistry.1986;25:5500-5506.

22. Maruyama K, Kennel SJ, Huang L. Lipid composition is important for highly efficient target binding and retention of immunoliposomes. Proc. Natl. Acad. Sci. USA. 1990;87:5744- 5748.

23. Mori A, Kennel SJ, Huang L. Immunotargeting of liposomes containing lipophilic antitumor prodrugs. Pharm. Res.1993;10:507-514.

24. Mori A, Kennel SJ, Waalkes MVB, Scherphof GL, Huang L. Characterization of organ-specific immunoliposomes for delivery of 3',5' -O-dipalmitoyl-5-fluoro-2'-

deoxyuridine in a mouse lung metastasis model. Cancer Chemother. Pharmacol.1995; 35:447-457.

25. Klibanov AL, Maruyama K, Torchilin VP, Huang L. Amphipathic polyethyleneglycols effectively prolong the circulation time of liposomes. FEBS Lett. 1990; 268:235-237.

26. Uster PS, Allen TM, Daniel BE, Mendez CJ, Newman MS, Zhu GZ. Insertion of poly(ethylene glycol) derivatized phospholipid into pre-formed liposomes results in prolonged *in vivo* circulation time. FEBS Lett.1996; 386:243-246.

27. Leffler MT, Adams R. Aminophenyl-2-oxazolines as Local Anesthetics. J. Am. Chem. Soc.1937;59:2252-2258.

28. Greenwald RB, Gilbert CW, Pendri A, Conover CD, Xia J, Martinez A. Drug delivery systems: water soluble taxol 2'-poly(ethylene glycol) ester prodrugs-design and in vivo effectiveness. J. Med. Chem. 1996;39: 424-431.

29. Mayer LD, Tai LCL, Bally MB, Mitilene GN, Ginsberg RS, Cullis PR.. Characterization of liposomal systems containing Doxorubicin entrapped in response to pH gradients. Biochim. Biophys. Acta.1990;1025:143-151.

30. Ablordeppey SY, Fischer JB, Glennon RA. Is a nitrogen atom an important pharmacophoric element in sigma ligand binding? Bioorg. Med. Chem.2000; 8:2105-2111.

31. Iden DL, Allen TM. *In vitro* and *in vivo* comparison of immunoliposomes made by conventional coupling techniques with those made by a new post-insertion approach. Biochim. Biophys. Acta.2001; 1513:207-216.

32. Bendas G. Immunoliposomes: a promising approach to targeting cancer therapy. BioDrugs.2001; 15:215-224.

33. Vingerhoeds MH, Steerenberg PA, Hendriks JJ, Dekker LC, Van Hoesel QG, Crommelin DJ, Storm G. Immunoliposome-mediated targeting of Doxorubicin to human ovarian carcinoma in vitro and in vivo. Br. J. Cancer.1996; 74:1023-1029.

34. Sugano M, Egilmez NK, Yokota SJ, Chen FA, Harding J, Huang SK, Bankert RB. Antibody targeting of Doxorubicin-loaded liposomes suppresses the growth and metastatic spread of established human lung tumor xenografts in severe combined immunodeficient mice. Cancer Res.2000; 60:6942-6949.

35. Goren D, Horowitz AT, Tzemach D, Tarshish M, Zalipsky S, Gabizon A. Nuclear delivery of Doxorubicin via folate-targeted liposomes with bypass of multidrug-resistance efflux pump. Clin. Cancer Res. 2000; 6:1949-1957.

36. Pan XQ, Zheng X, Shi G, Wang H, Ratnam M, Lee RJ. Strategy for the treatment of acute myelogenous leukemia based on folate receptor beta-targeted liposomal Doxorubicin combined with receptor induction using all-trans retinoic acid. Blood 2002; 100:594-602.

37. Figure Legends

Figure 1. The structures (A) and the synthesis schemes (B & C) for the targeted and non-targeted lipids.

Figure 2. Cellular uptake of fluorescent liposomes. Rhodamine-labeled liposomes, targeted or non-targeted, were added to DU-145 cells and the cellular uptake of liposome is examined 4 h later (A). In a separate experiment cells were pretreated with HP (30μM) for 2 h prior to addition of liposomes and liposome uptake was then similarly examined as described above (B). The results were expressed as arbitrary fluorescence unit per mg of cellular protein (n=3).

Figure 3. Uptake of rhodamine-PE labeled liposomes by DU-145 cells measured by Fluorescence microscopy. The left, middle and right columns correspond to the respective images of cells treated with liposomes containing 2 mol% of DSPE-PEG(2000)-OCH_3 (control), DSPE-PEG-SP3-AA and DSPE-PEG-SP2-AA, at a total lipid concentration of 6.4 μM (A), 19.3 μM (B) or 58 μM (C). Magnification 200X.

Figure 4. Cytotoxicity of DOX in different liposome formulations. DU-145 cells were incubated with various concentrations of free DOX or DOX encapsulated in liposomes containing DSPE-PEG-SP2-AA or DSPE-PEG(2000)-OCH_3. The viability of cells was measured 48 h later by MTT assay (A). In a separate experiment cells were treated with haloperidol (30 μM) for 2 h prior to addition of drugs and the cytotoxicity was then similarly examined as described above (B). n=3.

Figure 5. Uptake of rhodamine PE labeled liposomes by DU-145 tumors in mice. The top, middle, and bottom rows correspond to the respective fluorescence images of tumors at 2, 4 and 24 h post injection. The left, middle and right columns correspond to the respective images of tumors treated with HEPES buffer saline (control), liposome containing 2 mol% of DSPE-PEG(2000)-OCH_3, and liposome containing 2 mole% of DSPE-PEG-SP2-AA. Magnification 200X.

Figure 6. Uptake of DOX encapsulated liposomes by DU-145 tumors in mice. The top row corresponds to fluorescence images and the bottom row is the corresponding bright field images. The left, middle and right columns correspond to the respective images of tumors treated with HEPES buffer saline (control), liposome containing 2 mol% of DSPE-PEG(2000)-OCH_3, and liposome containing 2 mole% of DSPE-PEG-SP2-AA. Magnification 200X.

Figure 7. Inhibitory effect of anisamide-targeted liposomal DOX on the growth of DU-145 tumor. Groups of five mice were inoculated with DU-145 cells. Five days later mice received the following treatments at a DOX dose of 7.5 mg/kg: A) DOX-liposome containing DSPE-PEG(2000)-OCH_3 (black triangle); B) free DOX (black circle); and C) DOX-liposome containing DSPE-PEG-SP2-AA (white square). Control mice received HBS. Tumor sizes in each group were measured twice a week and compared. $p<0.05$ (vs DOX-liposome containing DSPE-PEG(2000)-OCH_3).

Figure 1A

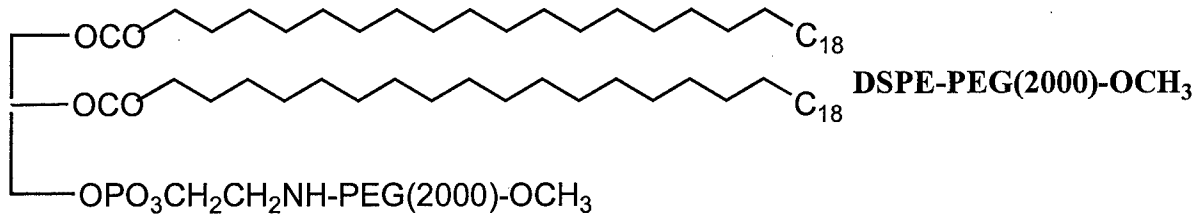

DSPE-PEG(2000)-OCH$_3$

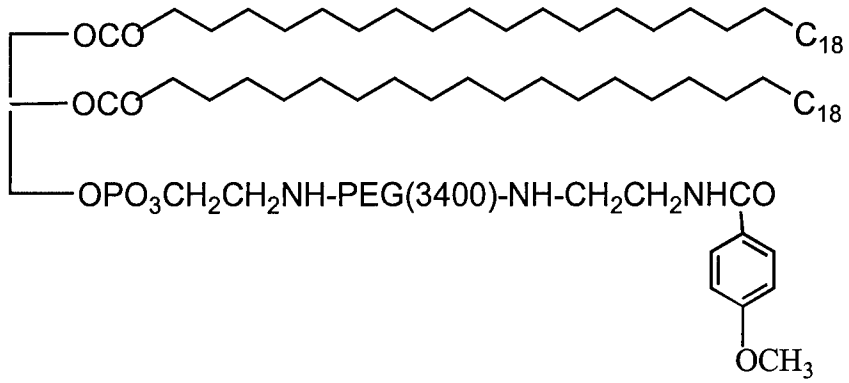

DSPE-PEG-SP2-AA

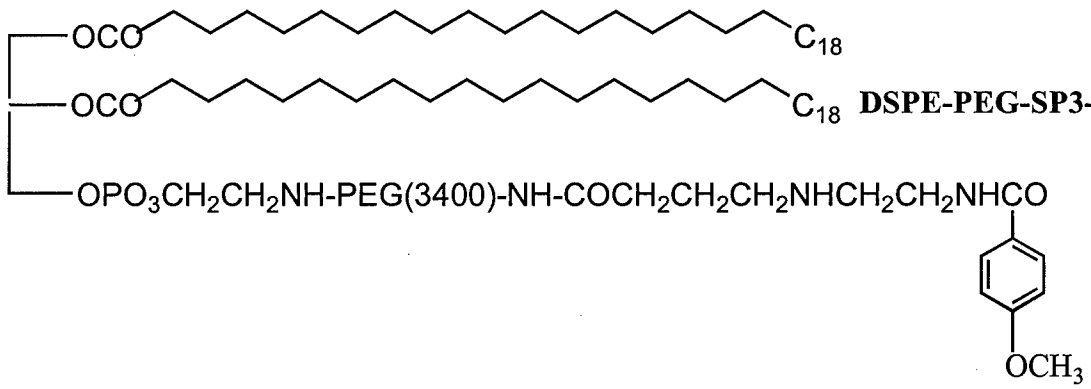

DSPE-PEG-SP3-AA

Figure 1B

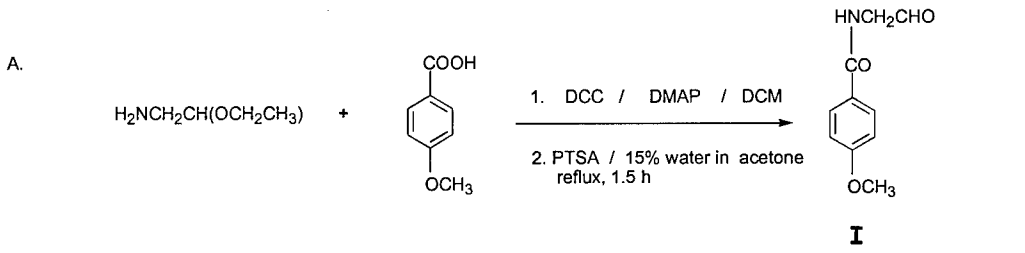
A.
$H_2NCH_2CH(OCH_2CH_3)$ +
COOH
OCH_3
1. DCC / DMAP / DCM
2. PTSA / 15% water in acetone
reflux, 1.5 h
$HNCH_2CHO$
CO
OCH_3
I

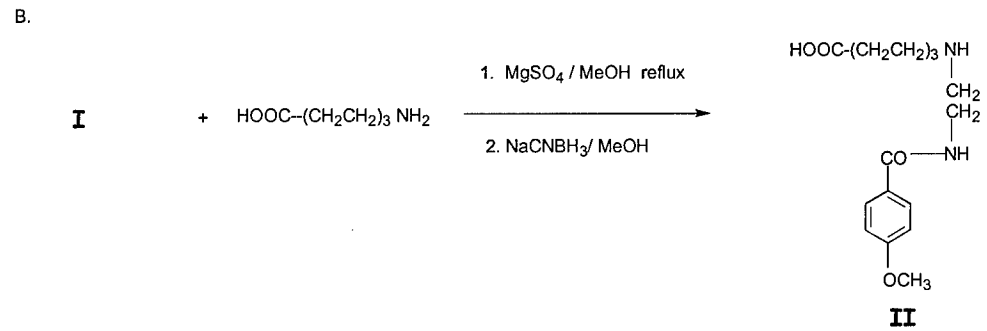
B.
I
+ $HOOC-(CH_2CH_2)_3 NH_2$
1. $MgSO_4$ / MeOH reflux
2. $NaCNBH_3$/ MeOH
$HOOC-(CH_2CH_2)_3 NH$
CH_2
CH_2
CO
NH
OCH_3
II

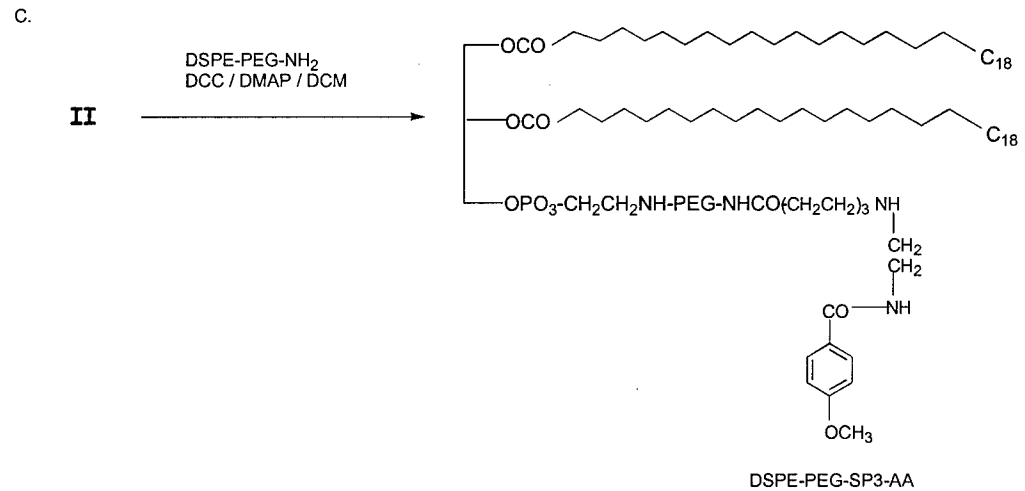
C.
II
DSPE-PEG-NH_2
DCC / DMAP / DCM
OCO
C_{18}
OCO
C_{18}
$OPO_3-CH_2CH_2NH-PEG-NHCO(CH_2CH_2)_3 NH$
CH_2
CH_2
CO
NH
OCH_3
DSPE-PEG-SP3-AA

Figure 1C

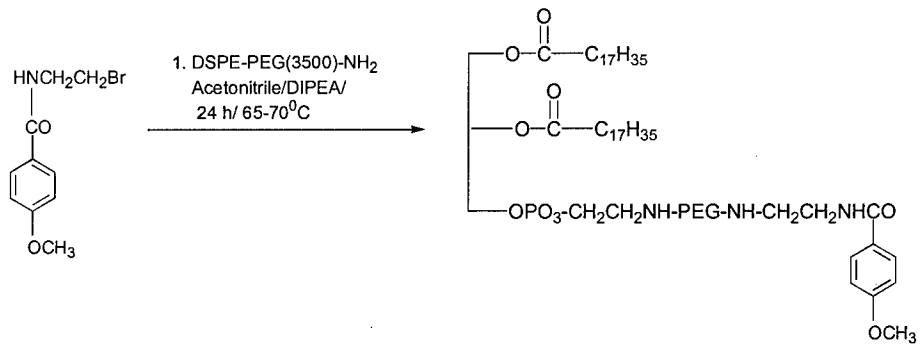

DSPE-PEG-SP2-AA

Figure 2A

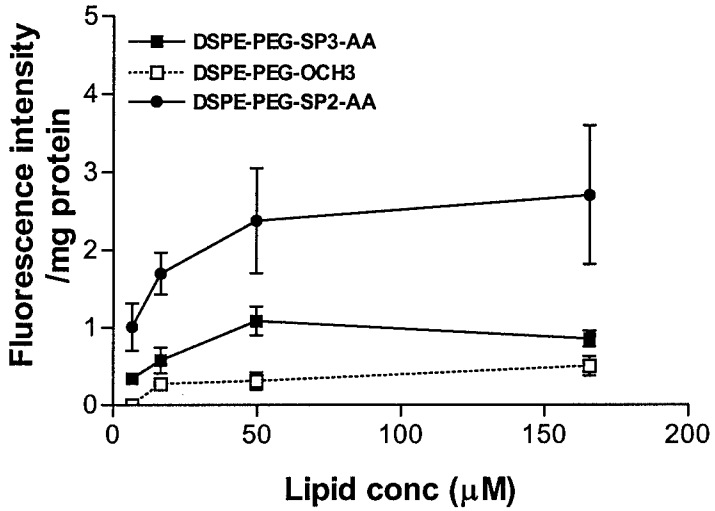
DSPE-PEG-SP3-AA
DSPE-PEG-OCH3
DSPE-PEG-SP2-AA
Fluorescence intensity /mg protein
Lipid conc (μM)
0
1
2
3
4
5
0
50
100
150
200

Figure 2B

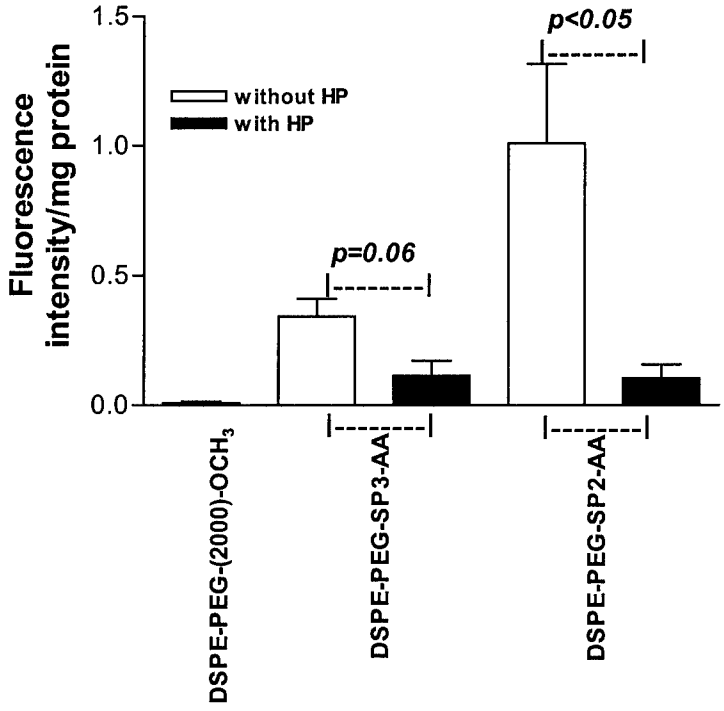
Fluorescence intensity/mg protein
1.5
1.0
0.5
0.0
without HP
with HP
p=0.06
p<0.05
DSPE-PEG-(2000)-OCH3
DSPE-PEG-SP3-AA
DSPE-PEG-SP2-AA

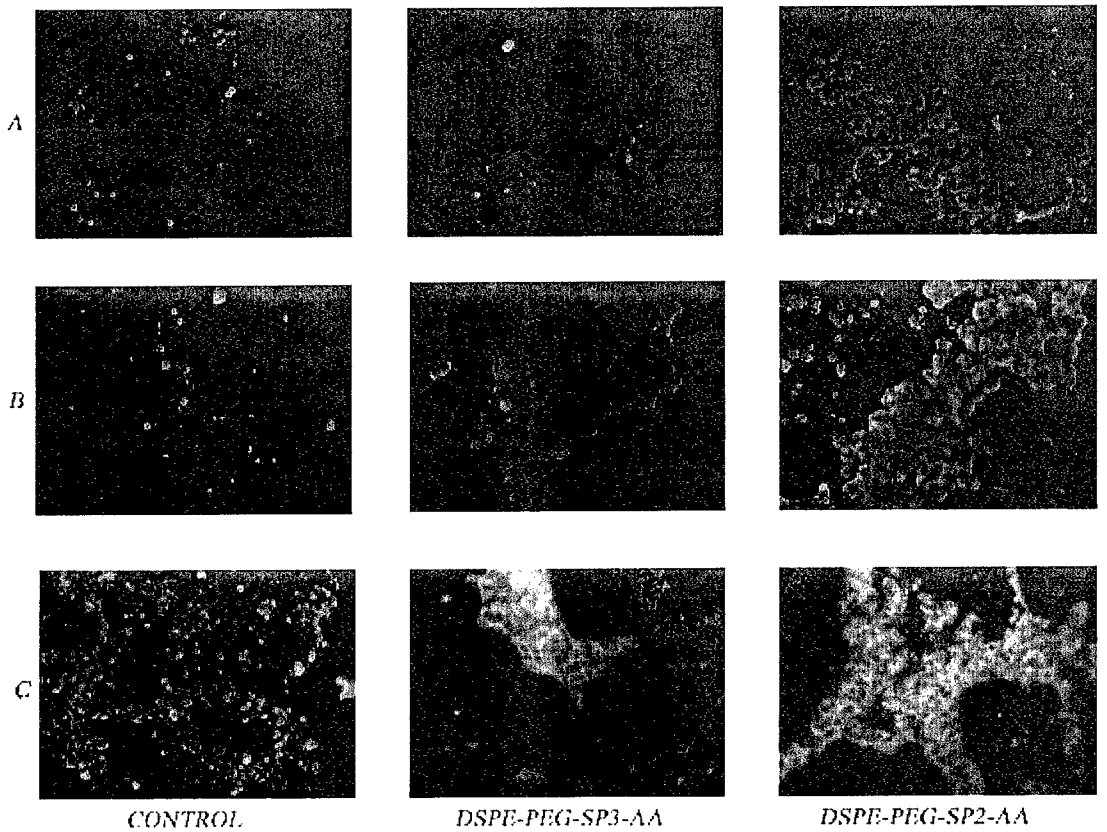
A
B
C
CONTROL
DSPE-PEG-SP3-AA
DSPE-PEG-SP2-AA

Figure 4A

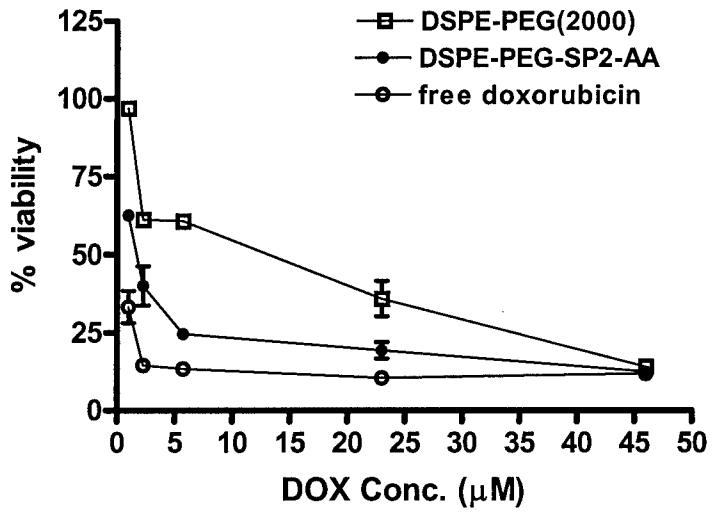
DSPE-PEG(2000)
DSPE-PEG-SP2-AA
free doxorubicin
% viability
125
100
75
50
25
0
0
5
10
15
20
25
30
35
40
45
50
DOX Conc. (μM)

Figure 4B

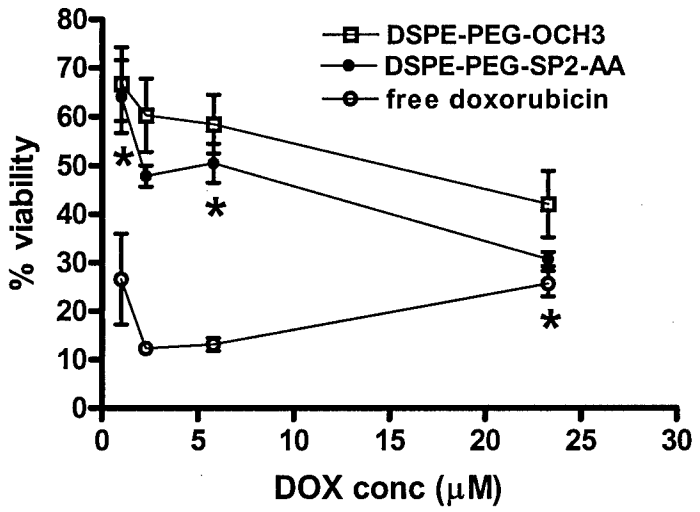
DSPE-PEG-OCH3
DSPE-PEG-SP2-AA
free doxorubicin
% viability
DOX conc (μM)
0
10
20
30
40
50
60
70
80
0
5
10
15
20
25
30
*
*
*

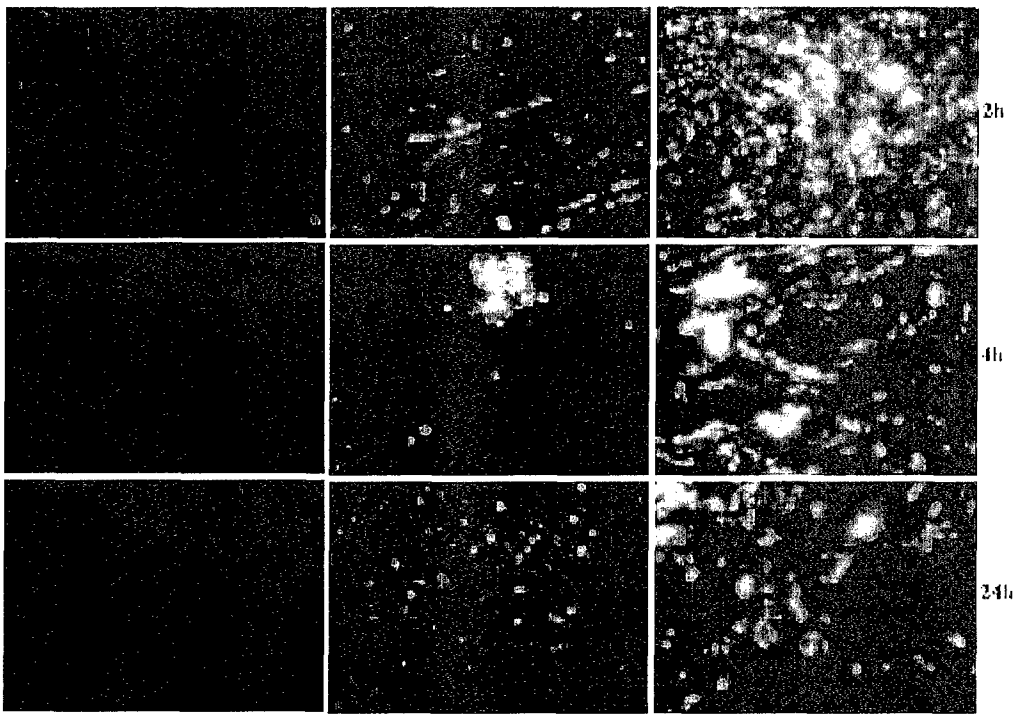

Untreated Control

Liposome with
DSPE-PEG(2000)-OCH3

Liposome with
DSPE-PEG-SP2-AA

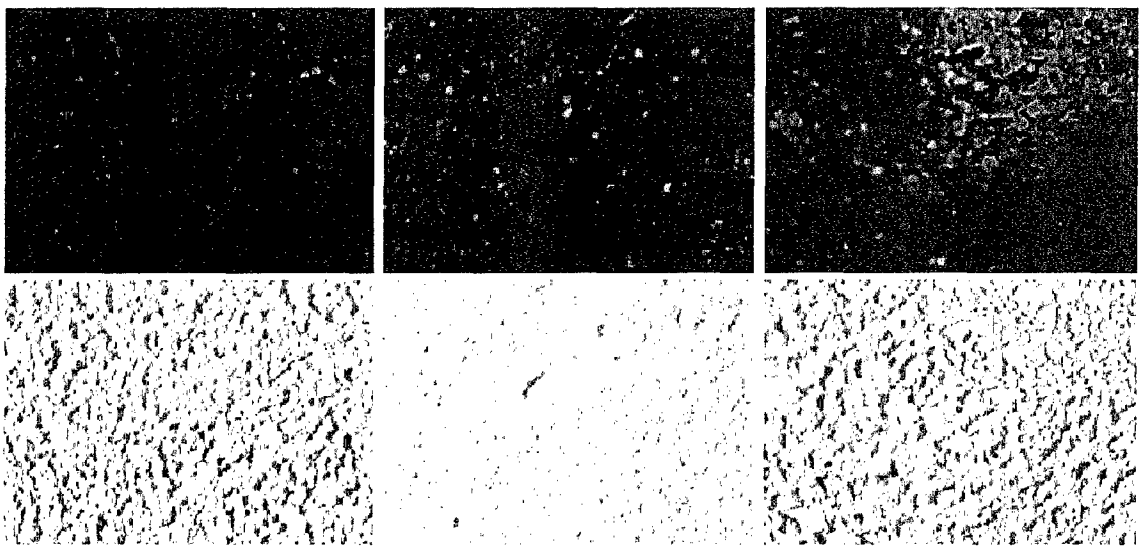

untreated control

liposome with
DSPE-PEG(2000)-OCH3

liposome with
DSPE-PEG-anisamide

Figure 7

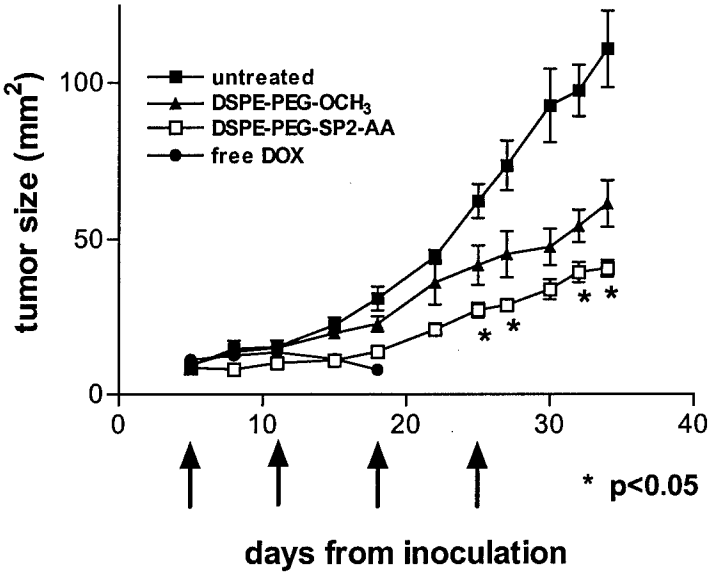
tumor size (mm^2)
100
50
0
untreated
DSPE-PEG-OCH$_3$
DSPE-PEG-SP2-AA
free DOX
0
10
20
30
40
* p<0.05
days from inoculation